Published in final edited form as:
J Comp Neurol. 2006 July 1; 497(1): 13–31.

Neonatal Deafness Results in Degraded Topographic Specificity (Frequency Resolution) of Auditory Nerve Projections to the Cochlear Nucleus in Cats

Patricia A. Leake*, **Gary T. Hradek**, **Leila Chair**, and **Russell L. Snyder**
Epstein Hearing Research Laboratory, Department of Otolaryngology - Head and Neck Surgery, University of California San Francisco, San Francisco, California 94143-0526

Abstract

We previously examined the early postnatal maturation of the primary afferent auditory nerve projections from the cat cochlear spiral ganglion (SG) to the cochlear nucleus (CN). In normal kittens these projections exhibit clear cochleotopic organization before birth, but quantitative data showed that their topographic specificity is less precise in perinatal kittens than in adults. Normalized for CN size, projections to anteroventral (AVCN), posteroventral (PVCN) and dorsal (DCN) subdivisions are all significantly broader in neonates than in adults. By 6–7 days postnatal, projections are proportionate to adults', suggesting that significant refinement occurs during the early postnatal period.

The present study examined SG projections to the CN in adult cats deafened as neonates by ototoxic drug administration. The fundamental organization of the SG-to-CN projections into frequency band laminae is clearly evident despite severe auditory deprivation from birth. However, when normalized for the smaller CN size in deafened animals, projections are disproportionately broader than in controls; AVCN, PVCN and DCN projections are 39%, 26% and 48% broader, respectively, than predicted if they were precisely proportionate to projections in normal hearing animals. These findings suggest that normal auditory experience and neural activity are essential for the early postnatal development (or subsequent maintenance) of the topographic precision of SG-to-CN projections. After early deafness, the basic cochleotopic organization of the CN is established and maintained into adulthood, but the CN is severely reduced in size and the topographic specificity of primary afferent projections that underlies frequency resolution in the normal central auditory system is significantly degraded.

Indexing terms

auditory deprivation; development; auditory nerve; cochlear nucleus; cochlear spiral ganglion; neonatal deafness; primary afferents; tonotopic organization; topographic maps

INTRODUCTION

Topographic maps are one of the fundamental organizing features of the central nervous system. In most sensory systems, the neighboring relationships of receptors in the sensory epithelium are maintained in their projections into the central nervous system. One major focus of developmental neurobiology over the past several decades has been on examining the

*Correspondence to: Patricia A. Leake, Ph.D., Epstein Laboratory, Dept. of Otolaryngology- H.N.S., Univ. of California San Francisco, 533 Parnassus Ave., Room U490, San Francisco, CA 94143-0526. Telephone: (415) 476-5958; FAX: (415) 476-2169, E-mail: leake@itsa.ucsf.edu.

developmental changes in specificity of these maps, the role of afferent input in the establishment and maintenance of these maps, and elucidating molecular cues that guide connectional selectivity (see Rubel and Cramer, 2002 for review). Many studies of visual system development have emphasized that competition driven by activity is essential for refinement of initial topographically imprecise neuronal projections into their precise adult patterns. For example, Simon and O'Leary (1992) reported that the retinal projections to the tectum in neonatal rats have terminal arbors that initially branch relatively widely over the tectum and which become much more topographically precise during subsequent development with "pruning" of the projections. Waves of correlated spontaneous neural activity have been recorded in the retina for some time before the onset of vision (Constantine-Paton et al., 1990; Maffei and Galli-Resta, 1990; Shatz, 1990; Goodman and Schatz, 1993; Feller et al., 1996), and it has been suggested that this neural activity is essential for the precise topographic organization of the visual system during early development. Recent studies have shown that specific spatiotemoral patterns of spontaneous and visual input guide the establishment of precise synaptic connections within the developing visual pathway (Zhou et al., 2003; Chiu and Weliky, 2003), and that the progressive refinement of visual receptive fields in the tectum involves a process of activity-dependent matching of the topography and strength of excitatory and inhibitory connections (Tao and Poo, 2005). Further, it has been suggested that such activity-driven processes shape refinement of neural connections throughout the nervous system (Schatz, 1990, 1996; Tao and Poo, 2005).

On the other hand, Chalupa and Snider (1998) reported that the retinotectal projections are topographically precise from the time retinal fibers first reach the tectum in embryonic and early postnatal ferrets. Many other recent studies also have emphasized the role of molecular cues in guiding the formation of precise topographic retinal projections to the tectum (O'Leary and Wilkinson, 1999; O'Leary et al., 1999). Specifically, it has been reported that a relatively precise retinotectal map forms during early development as a consequence of opposing gradients of the Ephrin proteins, with EphA3 receptors expressed in a temporalnasal gradient in the retinal ganglion cell axons and eph-A2 and eph-A5 expressed in opposing posterior-anterior gradients in the tectum (Cheng et al., 1995; Hansen et al., 2004). Thus, even in what is probably the best-studied of all topographic maps, the retinotectal map, the precise roles of -- and complex interactions *between*-- molecular mechanisms and neural activity in the formation and maintenance of spatially precise connections are still being elucidated. However, it is important to note that many examples have been reported where axons in the developing brain make initial connections that are very topographically precise, e.g., projections to the rat somatosensory cortex (Schlaggar et al., 1993; Schlaggar and O'Leary, 1994), and most recent studies have emphasized the role of molecular cues in guiding the early development of topographic selectivity. Eph/ephrin signaling is of particular interest in this regard because it has a well-established role in the formation of topographic maps in the central nervous system. In addition to the retinotectal projections (O'Leary and Wilkinson, 1999) Eph proteins also have a significant role in the development of topographic maps in the mammalian retinogeniculate pathway (Feldheim et al., 2000), in the thalomocortical projections of the somatosensory system (Prakash et al, 2000), and the glomerular map in the olfactory bulb (Cutforth et al., 2003). Moreover, several recent studies have suggested that the Eph proteins also play an important role in the establishment of topographic selectivity in the auditory pathways (See Cramer, 2005 for review; see Discussion)

Like the visual system, the auditory system in many mammals is very immature at birth, but precisely organized in adults. One of the principal features of this organization is tonotopy, the orderly arrangement of best frequency of the cochlear hair cells that is preserved within the cochlear spiral ganglion and in its projections centrally to the cochlear nucleus. In the normal adult cat each auditory nerve fiber sends collaterals to all three subdivisions of the cochlear nucleus (CN), and these projections precisely maintain the neighbor relationships of receptor

hair cells in the cochlea to form three separate tonotopic maps in the anteroventral (AVCN), posteroventral (PVCN) and dorsal cochlear nucleus (DCN). Moreover, each target cell group within each CN subdivision is characterized by synaptic connections with quite distinct morphologies. Thus, the auditory nerve provides an interesting model for examining molecular and activity-dependent mechanisms that may contribute to the formation of topographically precise connections and emergence of specific functional capacities.

Newborn cats are deaf, but by a few days postnatal the auditory nerve begins to exhibit some spontaneous activity, although discharge rates remain very low until about 10–14 days postnatal (mean <10 spikes/s as compared to rates up to 100 spikes/s in adults). In this early postnatal period only very high threshold responses with bursting and immature rhythmic discharge patterns are elicited in the auditory nerve in response to sustained acoustic stimuli (Walsh and McGee, 1987; Walsh and Romand, 1992; Fitzakerley et al., 1995; 1998). Fitzakerley et al. suggested that this immature activity resembles activity recorded in the retina during the refinement of retinotectal and retinogeniculate connections (Sretavan and Shatz, 1986; Simon and O'Leary, 1992; Wong et al., 1993; Shatz, 1996; Feller et al., 1996). Therefore, we previously hypothesized that auditory neurons innervating a restricted sector of the organ of Corti initially might form relatively broad CN projections, which would subsequently become more topographically restricted coincident with the emergence of adult-like frequency selectivity and sensitivity (Leake et al., 2002).

Other electrophysiological studies have provided detailed descriptions of specific aspects of functional development at several levels of the auditory system. The initial temporal response properties and the development of frequency selectivity, sensitivity and phase-locking have been described in the auditory nerve (Ehret and Romand, 1981; Dolan et al., 1985; see Walsh and Romand, 1992 for review), the cochlear nucleus and inferior colliculus (Kitzes, 1990) and the auditory cortex (Brugge et al., 1988, Bonham et al., 2004). Physiological and metabolic marker studies that have addressed directly the development of tonotopic organization at the level of the CN have reported clear tonotopic organization early in development, as soon as stimuli elicit a response (Ryan and Woolf 1988; Sanes et al. 1989; Webster and Martin, 1991; Friauf 1992; Friauf and Kandler, 1993). Anatomical studies have provided descriptions of the maturation of the organ of Corti and auditory periphery (for review, see Walsh and Romand, 1992; Sato et al., 1999), and our previous morphological studies provided details about the timing of emergence of the precise topography of connections from the developing cochlea to the CN. For this work we used the neuronal tracer Neurobiotin™ (NB) and made focal extracellular injections into the cochlear spiral ganglion (SG), which allows direct examination of projections from restricted sectors of the SG (representing a narrow range of frequencies in the adult) into the CN. These earlier studies demonstrated a highly precise topographic order in CN projections in kittens as young as six days postnatal (P6) (Snyder and Leake, 1997). Labeled axons and terminals formed discrete "frequency band laminae" within the anteroventral (AVCN), posteroventral (PVCN), small cell cap and dorsal (DCN) divisions of the cochlear nucleus complex, and when the dorsal-to-ventral thickness of these bands (distribution across the frequency gradient) were measured and normalized for the size of the CN, the projections at P6 or P7 were as precise as those in adults. A subsequent study examined the earliest postnatal and late gestational periods (Leake et al., 2002), demonstrating that the SG-to-CN projections exhibited clear tonotopic organization in neonates, and even in animals examined after Caesarian section performed up to 5 days before birth. However, quantitative data revealed that the topographic restriction of projections into frequency band laminae was less precise in all 3 CN subdivisions in perinatal kittens than in older kittens or adults. Normalized for CN size, the projections to the AVCN were >50 % broader and projections to both the PVCN and DCN were >30% broader in neonates. Thus, significant refinement in connectional specificity occurs during the early postnatal period and is complete by about P6–P7. This means that the precise topographic map of the cochlear receptor epithelium in the CN

is fully established for as much as several days before adult-like frequency selectivity and sensitivity are recorded in the auditory nerve (at about P21), and refinement of CN projections occurs at the time spontaneous activity is emerging and very immature bursting and rhythmic responses to high intensity acoustic stimuli are elicited in the auditory nerve of cats (Fitzakerley et al., 1995; 1998).

The present study examines the consequences of *early profound hearing loss* upon the topographic organization of the SG projections and their refinement during the early postnatal period. Our hypothesis is that normal cochlear function (spontaneous and driven activity in the auditory nerve) is required for the topographic refinement of the primary afferent inputs to the central auditory system. A corollary of this hypothesis is that the connectional selectivity of SG to CN projections will be degraded in animals that are deafened early in life. SG injections were made in adult cats that had been deafened by ototoxic drug administration beginning immediately after birth. The objectives were to determine whether the normal cochleotopic organization of the SG projections to the CN, which underlies frequency selectivity in the normal auditory system, is established and maintained into adulthood after severe auditory deprivation early in life, and whether the CN frequency band laminae achieve full refinement and precision in these neonatally deafened animals.

MATERIALS AND METHODS

Experimental Animal Groups; Deafening Procedure

All procedures involving animals were approved by the Institutional Animal Care and Use Committee at the University of California, San Francisco and conformed to all NIH guidelines. Sixteen animals were included in this study, and all were bred in a closed colony maintained at the University of California San Francisco. Female cats were bred for periods of ≤24 hours, so the gestation period for each litter was known within +/− 24 hours. The mean gestation period in our colony is 65 days.

Kittens are unresponsive to sound at birth due to the immaturity of the auditory system (for review, see Walsh and Romand, 1992). Ten of the animals included in this study were deafened as neonates by daily injections of the ototoxic aminoglycoside antibiotic, neomycin sulfate (60 mg/kg, I.M., S.I.D.), beginning the day after birth and continuing for 16–30 days during the period when nearly adult-like hearing sensitivity would normally develop. Profound hearing loss was confirmed by auditory brainstem responses (ABR) testing as described previously (Leake et al., 1999). Briefly, animals were tranquilized with inhaled isoflurane (3% via mask for induction; 1–2% for maintenance) and placed in a double-walled sound-attenuating chamber. A hollow tube was inserted into the external auditory meatus and auditory stimuli were delivered through a headphone speaker (STAX-54) enclosed in a small chamber connected to the tube in the ear canal. The sound delivery system was calibrated with a sound level meter (Bruel and Kjaer 2209), and thresholds were determined for ABRs to clicks by averaging responses for 500 presentations of stimuli. Animals were first tested after 16 days of neomycin administration, and injections were discontinued as soon as each animal exhibited thresholds higher than the maximum output of the system (>105 dB). If residual hearing was observed, neomycin injections were continued in 2–3 day increments, and the animal was tested again after each series of injections until there was no response. Most animals exhibited profound hearing losses by 20 days of injections, but 2 animals still had small amounts of residual hearing after 24 days. In these 2 subjects, the neomycin dosage was increased to 70 mg/kg, and both exhibited profound hearing losses after 6 additional days of treatment. A previous investigation has demonstrated that profound hearing losses induced by this method are associated with virtually total degeneration of the cochlear hair cells (Leake et al., 1997).

Table 1 shows the individual deafening histories and the number of SG injections made in the 10 deafened animals included in this study. The first experimental group (5 animals) was studied at 3–5 months of age as young adults. In normal-hearing animals at this age, the CN would have achieved its full adult size (Larsen, 1984). SG injections were made bilaterally in this first group. In addition, data were obtained from a second experimental group of 5 neonatally deafened animals that had received a cochlear implant unilaterally (in the left cochlea) at 6 to 9 weeks of age as part of another study and underwent several months of chronic electrical stimulation delivered by the implant. In these subjects, SG injections were made only in the deafened, non-implanted right cochleae to examine the SG-to-CN projections. Control data were obtained from 4 normal adult cats (8 CN).

Neurobiotin™ Injections

All animals were free of middle ear disease as judged by direct examination of the middle ear and auditory bulla. Animals were tranquilized initially with isoflurane. An intravenous catheter was then inserted into the cephalic vein, and a surgical level of anesthesia induced and maintained by infusion of sodium pentobarbital (20–40 mg/kg, to effect). Respiratory rate, heart rate and body temperature were monitored throughout the experimental procedures. Body temperature was maintained using a warm water recirculating blanket. The auditory bulla was exposed surgically and opened, and the round window membrane of the cochlea was excised to allow direct visualization of Rosenthal's canal in the hook region and lower basal turn. For each injection, a small opening into the bone of the modiolus overlying Rosenthal's canal was made using the tip of a 30-gauge needle as a curette.

Injections of the neuronal tracer neurobiotin™ (NB; from Vector Laboratories, Burlingame, CA) were made using thick-walled glass micropipettes with tips broken to a diameter of ≈10–30 μm. The pipettes were mounted on a 1μl microsyringe (Unimetrics) and sealed in place with melted dental wax. Micropipettes were filled with a solution of 5% NB dissolved in distilled water. A small quantity of the vital dye Trypan blue (<0.5%) was added to the clear NB solution so that the injections could be visually confirmed. The microsyringe was mounted in a micromanipulator. The pipette tip was positioned over a selected site and inserted into the spiral ganglion. A small quantity of the NB (≈0.5 μl) was injected using manual pressure on the syringe plunger (or in later experiments, a micromanipulator was used to advance the plunger). The tip of the pipette was left in place for a minimum of 10 minutes to allow the tracer to diffuse into the ganglion.

In most cases injections were made at two locations (frequency ranges) in each cochlea, and in one control subject, 3 injections were made in one cochlea. The locations of injections were recorded, and the round window was sealed with a small disk of gelfilm™ (Upjohn) or Saran™ wrap (Dow Corning). The incision was sutured closed, and animals were maintained sedated for post-injection periods of 8 to 12 hours to allow sufficient time for the tracer to be transported to the CN.

Preparation of Cochlear Specimens

Fixation, NB cytochemistry, embedding and sectioning for light microscopy— After the postinjection period, animals were deeply anesthetized with sodium pentobarbital (20–40 mg/kg IV, to effect), and the cochleae were gently perfused with a mixed aldehyde fixative (2.5% paraformaldehyde and 1.5% glutaraldehyde in 0.1M phosphate buffer at pH 7.4) introduced through the round and oval windows. Then an overdose of sodium pentobarbital (100 mg/kg) was administered, and transcardiac perfusion was carried out using 5% lactated Ringer's followed by fixative (0.5% paraformaldehyde, 2.5% glutaraldehyde, and 4% sucrose in 0.1M phosphate buffer at pH 7.4). Following perfusions, the brain and temporal bones were removed for histology.

The otic capsule bone of the cochlea was thinned with a diamond dental burr until the stria vascularis was clearly visible throughout the cochlear spiral. The dissected cochlea was post-fixed in 1% phosphate-buffered osmium tetroxide (with 1.5% potassium ferricyanide added to enhance contrast). After rinsing in buffer, the specimen was placed in 0.1M EDTA for 18 hours to partially decalcify the modiolus. The otic capsule of the hook region and the lower basal turn was then dissected, removing the lateral aspect of the bony canal to expose the scala vestibuli and the stria vascularis. Next, additional microdissection was done to isolate and remove the hook region and the lower basal coil, including the adjacent modiolus containing the spiral ganglion with the NB injection sites, which were located in this basal region. These isolated specimens were agitated on a rotator for 2 hours in 2% dimethylsulfoxide DMSO, which acted as a cryoprotectant during the next step, in which specimens were rapidly frozen in Freon R134A cooled with liquid nitrogen. These additional steps of dissection and freezing are necessary to facilitate penetration of the cytochemical reagents, since the relative impermeability of the tissue surrounding Rosenthal's canal otherwise prevents adequate penetration. After freezing, the isolated cochlear pieces containing the injection sites were rinsed in Tris-HCL buffer (pH 7.6; Sigma) for 15 minutes to quench aldehydes, rinsed in phosphate buffer (0.1M at pH 7.4) and placed in VECTASTAIN™ ABC reagent solution from Vector Laboratories for 12 hours at 4° C.

The NB/ABC complex was demonstrated using 3,3′-diaminobenzidine tetrahydrochloride (DAB) (Sigma) substrate with cobalt intensification as follows. Specimens were soaked for 30 minutes in 0.5% CoCl in Tris, rinsed in Tris and transferred back to phosphate buffer (0.1 M at pH 7.4). Next the specimens were preincubated for 30 minutes in 0.1% DAB dissolved in phosphate buffer (final pH, 7.0), followed by incubation in two changes (1.5 hours each) of the same DAB solution with the addition of 0.1% hydrogen peroxide. All steps were carried out with continuous agitation on a rotator.

After cytochemical processing, the specimens were dehydrated and embedded in LX™ epoxy resin along with the remainder of the cochlea. Extra-thick surface preparations were then made as follows. Halfcoils of the cochlea, which contained both the organ of Corti and the adjacent spiral ganglion, were isolated and mounted in LX on glass slides. The half-coil pieces were cut into smaller segments as necessary to orient the basilar membrane flat and in a plane parallel to the slide. The basilar membrane was then measured from base to apex along the tops of the pillar cells and was marked in increments of 0.5mm. Small segments (<0.5 mm) of the organ of Corti along with the associated spiral ganglion were excised at intervals of about 2 mm throughout the cochlea. Blocks containing <0.5 mm of the organ of Corti and its adjacent spiral ganglion were removed from the surface preparation at 2 mm intervals, using cuts made in an axis parallel to the radial nerve fibers. These pieces were re-mounted, and semi-thin sections (1–2μm) were cut in the radial plane and stained with Toluidine blue. Sections were collected at 50 μm intervals for evaluation of spiral ganglion survival in the deafened cochleae. Additional blocks were prepared in the region(s) where the NB injection site(s) were identified, and serial sections were collected throughout the region containing damaged and labeled neurons.

Analysis of injection sites—Sections through cochlear injection sites were examined in the light microscope (Axioskop 2). High resolution video images (2584 × 1936 pixels) for illustrations were acquired using Photoshop 5.0, a Kodak digital camera, and a PC. For calibration, an image of a micrometer scale was captured and superimposed on the image of the histological section.

In our previous studies examining the SG projections to the CN, the extent of each NB injection site in the spiral ganglion was defined by the distributions of labeled afferent fibers and terminals innervating inner hair cells in the organ of Corti (Snyder et al., 1997; Snyder and

Leake 1997; Leake et al., 2002). However, this was not possible in the neonatally-deafened animals in the current study because all the cochlear hair cells had degenerated, and many (or most) of the peripheral radial nerve fibers within the osseous spiral lamina had also degenerated. In addition, our previous studies showed that due to the relative impermeability of Rosenthal's canal, penetration of cytochemical reagents was frequently inadequate to demonstrate NB reaction product in the SG. Therefore, the location and size of all injection sites were defined by additional criteria in serial sections through the region, including evidence of penetration of the pipette into Rosenthal's canal, and the distribution of damaged, pyknotic and missing SG cell somata. The locations and extents of injection sites were defined initially by absolute distance in mm from the basal end of the cochlea. To estimate the represented frequencies of the labeled neurons projecting to the CN, the total basilar membrane length for each cochlea was used to calculate positions of injection sites as a proportion of basilar membrane length (% distance from base). The represented range of frequencies encompassed by each injection was then calculated using Greenwood's frequency-position function (Greenwood, 1974, 1990) with the revised constants suggested by Liberman (1982) for the cat cochlea.

Preparation of Cochlear Nucleus Sections and Analysis of NB-Labeled SG-to-CN Projections

Preparation of CN sections and NB cytochemistry—Following transcardiac perfusion, the brain stem (rostral midbrain to the caudal medulla) was isolated, rinsed in Ringer's solution and placed in two changes of 40% sucrose in 0.1M phosphate buffer at pH 7.4 at 4° C for at least 72 hours until saturated. The right side of the brain was marked, specimens were frozen rapidly using dry ice, and serial coronal sections were cut at a thickness of 50 μm. The sections were washed in 3 changes of 0.05M TRIS buffer (pH 7.6) followed by three changes of phosphate buffer. Then the sections were incubated in VECTASTAIN" ABC reagent solution from Vector Laboratories for 12 hours at 4° C and rinsed in 3 changes of 0.05M TRIS buffer. For the demonstration of the NB/ABC complex, the sections were placed in a solution consisting of 20 mg of 3,3′-diaminobenzidine tetrahydro-chloride (DAB; Sigma), 1 mg cobalt chloride, and 1 mg nickel ammonium sulfate in 100 ml TRIS buffer. After 30 minutes of pre-incubation, the sections were transferred to a fresh solution of the DAB solution with one drop of 3% hydrogen peroxide added, and incubated for an additional period ranging from 60–120 minutes until we observed clear evidence of background staining in sections examined under the microscope. Any additional incubation of sections beyond this point will degrade the signal by increasing the background noise resulting from staining of endogenous peroxidases present in the tissue. The sections were then washed in 3 changes of TRIS buffer, transferred to phosphate buffer and mounted on gelatinized slides. The slides were dried, dehydrated through graded alcohols, cleared in xylenes, and cover-slipped using Permount™. Tissue shrinkage has been evaluated previously by direct measurements made in wet sections and repeated in the same sections after drying on the slide, and repeated again after clearing and mounting. Mean shrinkage was less than 0.5% in brains processed in this manner (Leake et al., 2002).

CN cross-sectional area measurements; scaling factor—In order to evaluate the overall change in size of the CN in deafened animals, CN cross-sectional areas were determined. A series of measurements was made to determine the maximum cross-sectional area of the CN in sections just posterior to the auditory nerve root entry zone in each case (Leake et al., 2002). Sections were imaged digitally and measured at a resolution of approximately 6.5 μm/pixel (640 × 480 =4.18 mm × 3.13 mm) in ImageJ 1.34N software. The perimeter of the CN was outlined using the tracing tool, and the area was calculated using the area function. The values thus obtained for the cross-sectional areas were used to compare CN size in deafened vs. normal groups using an unpaired Student's T-test (with the Bonferroni correction factor).

In addition, in order to normalize the measurements of labeled auditory nerve projections relative to the smaller size of the CN observed in deafened animals, a single dimensional measurement of the dorsal-to-ventral height of the CN (i.e., across the frequency gradient of the CN and orthogonal to the long axis of the auditory nerve projection laminae). Measurements were made in the largest section containing a clear PVCN lamina just caudal to the bifurcation of fibers ascending to the AVCN. Using the line function in ImageJ, the longest possible line was drawn that passed orthogonally through the PVCN projection lamina and intersected the dorsal and ventral boarders of the CN. In order to normalize for the smaller size of the CN in deafened animals, a scaling factor was calculated by dividing the CN height in each deafened subject by the average normal CN height. This value was multiplied by the average normal projection thickness (for each CN subdivision) to calculate "predicted values" for the projection laminae in each deafened subject –that is, the thickness of the projections expected in each individual deafened subject if the deafened CN and its projections were precisely proportional to those in the normal controls. Statistical comparison and deafened and control groups were made using the Student's T-test (upaired).

Measurements of CN projection laminae—The nomenclature used here for the cytoarchitectonic subdivisions and cell types of the cochlear nucleus follows that of Osen (1969, 1970) since smaller subdivisions defined by others in Golgi material (Brawer et al, 1974; Cant and Morest, 1984; Tolbert and Morest, 1982) are difficult to identify in our unstained sections reacted for NB labeling. For descriptions of labeled fiber and synaptic terminal morphology, the terminology of Rouiller et al. (1986) was adopted. For quantitative analysis of projection patterns, digital images were captured at a resolution of approximately 1 μm/pixel (640×480 pixels = 0.640 mm × 0.480 mm) for all measurements in AVCN and PVCN and DCN. The thickness of each lamina of labeled axons and terminals (its height across the frequency gradient) was measured using the "profile scan" analysis function of the NIH Image software (version 1.63). Measurements were made in each CN subdivision, in serial sections selected throughout the main development of each projection (sections at the rostral and caudal extremes of the laminae were eliminated from analysis to avoid tangential measurements). The projection thicknesses were measured orthogonal to the plane of the individual CN projection lamina, in order to estimate the distribution of labeled fibers across the frequency gradient within each respective subdivision. Thus, AVCN and PVCN laminae were measured orthogonal to their long axis, and the DCN projections were measured in an axis parallel to the pial surface. The scans were always executed beginning at the low frequency side of the laminae (i.e., from ventral to dorsal) and using a window that was 0.05 mm in width and no less than 0.4 mm in length. Three scans were made in each image, and all images with clear projections were analyzed, so that on average about 90 scans were included in the analysis of the projection(s) to each CN (see Results, "Measurements of CN Projection Laminae"). To determine projection thickness, all scans for a given projection were averaged, and average pixel density was displayed as a function of distance across the 0.4 – 0.8 mm window. The threshold then was set at a level at which some negative values occurred on both sides of the pixel-density peak formed by the projection(s) within the window. The point at which the first negative number appeared was then determined on each side of the peak, and the total pixel density value for all bins between these 2 points was assigned a value of 100% by dividing each bin by the total pixel density value. Finally, the minimum distance containing 90% of the total pixel-density was determined and defined as our estimation of projection thickness. All statistical analysis was performed using SigmaStat v.2.03 software. A one way ANOVA Tukey Test, was used for statistical comparisons of projections in deafened and control subjects. The same test also was used to compare the projection thickness in deafened subjects with the "predicted" thickness (i.e., if projections in the smaller CN of deafened subjects were precisely proportionate to those of equivalent projections in normal controls). These predicted values were calculated by multiplying the average projection thickness measured in each CN

subdivision in normal controls by the scaling constant (the dorsal-to-ventral height of the individual CN section with the maximum CN cross-sectional area observed in each deafened subject, divided by the mean height of the CN in the normal adult group).

In CN that had double projections from 2 injections made in a single cochlea, the distance separating the 2 projection laminae was also determined by measuring the distance between the 2 maxima in the mean pixel density function in all sections in which the 2 distinct projections were measurable. Finally, the density of NB labeled projections was determined by measuring the mean pixel density in the average of all scans for a given projection and dividing by the mean width of that scan to provide a mean pixel-per-mm value for each projection.

Photomicrograph images for illustrations were captured using Axiovision AC software (v. 4.2.0.0) as tiff files at a resolution of 2584 × 1936 pixels. Images were imported into Photoshop (v. 8) or Canvas (v.9) to add labels and scale bars. In addition, in some images background subtraction was used and contrast and brightness were adjusted to match images that appeared in the same figure.

RESULTS

Spiral Ganglion Cell Degeneration

Figure 1 illustrates the time course of degeneration of spiral ganglion (SG) neurons in a large group of animals (including, but not limited to, subjects in the current study) that were deafened as neonates using the neomycin protocol employed in the current study. There is a significant correlation between the overall survival of the SG neurons (SG cell density averaged throughout the cochlea) and the duration of deafness for this large group (r^2=0.75), although considerable variability is noted among subjects examined at any specific interval post-deafening. The deafened animals in the current study ranged in age from 14 to 41 weeks at the time of study. By the time of study, examination of histological sections throughout the cochleae showed that all the cochlear hair cells had degenerated, many (or most) of the peripheral radial nerve fibers within the osseous spiral lamina had degenerated, and significant degeneration of the SG was observed in the cochleae of these deafened animals. The first experimental group had a mean age at the time of the study of about 16 weeks (4 subjects for which SG data were available), and the mean spiral ganglion cell density (averaged throughout the cochlea) was 55.8 % of normal (Fig. 2A). The second group of animals was older than the first, with a mean age of about 33 weeks when they were studied, and the average SG density was 44.3% of normal (Fig. 2B), about 11% lower than the first group, as expected due to the longer duration of deafness. Although there was also some variation in ganglion cell survival in different cochlear regions, average survival in the basal cochlea where NB injections were made was about 59% and 45% of normal, respectively in the two groups, similar to their overall averages.

Analysis of Injection Sites

Again, examination of histological sections throughout the cochleae showed that there were no hair cells present in any of the deafened animals. Thus, it should be emphasized that the “represented frequencies” of injections were calculated in the deafened animals only for the purpose of comparing cochlear location and injection size to the normal control group, and these values are not meant to imply that the organ of Corti was functional in the deafened animals. Further, since frequency calculations are based upon percentage of basilar membrane length, it is important to note that the mean basilar membrane length in the deafened group was 24.8 mm. and was not significantly different from normal adult cats (24.6 mm). This finding is consistent with our previous study which demonstrated that the basilar membrane/

organ of Corti length in neonatal kittens studied at P0–P1 is not significantly different from that of adult cats (Leake et al., 2002; see Table 2). Thus, the basilar membrane is already full adult length at the time we begin administration of the ototoxic drug injections in the present study, and it is not surprising that its value is normal in the deafened animals studied as adults.

The extent of each injection site was determined in serial sections that were evaluated for evidence of the penetration of the NB pipette into Rosenthal's canal and damaged or missing spiral ganglion cells (Fig. 3A,B). The values obtained were averaged for subjects in each animal group for the comparison of injection site size (Fig. 3C). Since injections were made through the round window, injection sites were limited to relatively high frequency (basal) positions ranging from ≈1.5 to 6.5 mm from the base, equivalent to a frequency range of approximately 45 kHz to 15 kHz in the normal adult cochlea of the cat (Greenwood, 1974; Liberman, 1982). In most cochleae, 2 injections were made at loci that were separated as widely as possible within the accessible frequency range. These restricted injections labeled small clusters of SG neurons that normally would innervate cochlear sectors estimated to range in length from about 300 μm to 1.0 mm. Injections made in deafened animals averaged about 400 μm and were not significantly different from those in normal controls (Fig. 3B). In the normal adult cat, there are about 100 inner hair cells per mm of basilar membrane distance (Liberman, 1982), and a mm of basilar membrane is innervated by a sector of the spiral ganglion approximately 0.6 mm in length in these basal cochlear regions (Keithley and Cronin-Schreiber, 1987). Therefore, these injections labeled ganglion cells that would normally innervate about 70 inner hair cells on average. It should be noted that in our previous studies of normal kittens and adult cats, the distribution of NB-labeled profiles contacting the inner hair cells was evaluated as a more precise method of defining the frequencies represented by labeled neurons. In the deafened animals, however, the degeneration of terminals and radial nerve fibers that occurs following hair cell degeneration made this measure inappropriate for the current study, and additional criteria were required to estimate injection size as described above.

Measurements of CN Cross-Sectional Areas

The relative size of the CN was estimated in all cases by selecting the single largest section found just posterior to the entry of the auditory nerve and tracing the perimeter of the nucleus in digitized images as illustrated in Figure 4A. The cross-sectional area of the section was then calculated using Image software. In normal controls, the CN maximum area ranged from 6.42 to 7.21 mm^2 and the mean was 6.83 mm^2. In the individual deafened animals, the CN area values varied from 4.05 to 6.08 mm^2 (Table 1). The area values calculated separately for the two deafened groups showed that the CN cross-sectional areas were virtually identical (Fig. 4B) with mean values of 4.84 and 4.94 mm^2. Thus, the cross-sectional area of the CN was significantly smaller in the deafened animals and was, on average, only 71–72 % that of the CN in normal controls (Fig. 4C).

In addition, the dorsal-to-ventral height of each CN was measured in an axis orthogonal to the CN projection laminae, in the same dimension across which the CN projection laminae measurements were made (Fig. 4D). The control CN averaged 4.43 mm in height, as compared to 3.66 mm for the CN in deafened subjects, and the difference between the two groups was highly significant (Student's T-Test, unpaired). These values were used to normalize CN projection thickness for the difference in CN size between the two groups. If CN projections in the deafened subjects were proportionately smaller than projections in the normal CN, the thickness of the labeled laminae in deafened subjects would be expected to be, on average, 82.6% (3.66/4.43) of those in normal controls.

It should be noted that the individual data indicate substantial intersubject variability in the CN size among the deafened subjects comprising both groups (Table 1), but CN size was not correlated with age in these animals ($p=0.56$), which ranged from about 14 to 41 weeks of age

(Table 1). This finding supports the assumption that the CN had completed its full growth in the first (younger) of the two deafened groups. On the other hand, it also indicates that the longer duration of deafness in the second group was not associated with further reduction in CN size.

Characterization of NB-Labeled CN Projections

In the neonatally deafened animals, the major subdivisions of the CN were still clearly defined and identifiable by their cytoarchitecture. The NB-labeled central axons passed from the SG through the auditory nerve to the CN in discrete fascicles of intensely labeled axons that projected to all three major subdivisions of the CN. The labeled auditory nerve fibers entered the cochlear nerve root and bifurcated into ascending and descending branches. The ascending branches projected rostrally through and terminated within the anteroventral cochlear nucleus (AVCN). The descending branches projected caudally and terminated within the posteroventral cochlear nucleus (PVCN), and fine collaterals of these axons projected dorsomedially to the dorsal cochlear nucleus (DCN). These central projections, including the fine fibers projecting to the DCN, appeared to be fully labeled at post-injection times as short as 7 hours. Moreover, injections in deafened animals resulted in discrete bands or laminae of labeled fibers and terminals that exhibited a clear and normal tonotopic organization. That is, SG injections placed at more basal (higher frequency) locations resulted in projection laminae that were more dorsally positioned in each CN subdivision, whereas more apical injections resulted in labeled laminae that were positioned more ventrally in the CN (Figs. 4,5,6), as described previously in normal cats and kittens (Leake and Synder, 1989; Snyder and Leake, 1997;Snyder et al., 1997;Leake et al. 2002)

The characteristics of primary afferent fibers and terminals in normal cats as demonstrated by HRP labeling have been described in detail previously (see Ryugo and Fekete, 1982; Fekete et al., 1984; Roullier et al., 1986; Leake and Snyder, 1989; Snyder et al., 1997; Leake et al., 2002). The axons of passage and preterminal axonal ramifications in many of the neonatally deafened CN appeared somewhat less dense (i.e., had fewer fibers) and paler (fibers less intensely labeled) in all subdivisions of the cochlear nucleus than those seen in the controls (Figure 5). Nevertheless, numerous calyceal endings were identified in deafened projections to the AVCN (Fig. 5B), which largely corresponded in appearance to the endbulbs of Held seen in normal controls (Fig. 5A) and as described previously by Ryugo and Fekete (1982) and Limb and Ryugo (2000). In the PVCN, the labeled projections consisted of a felt-work of pre-terminal axons and larger axons of passage with occasional simple bouton and en passant swellings. The fine pre-terminal arborizations appeared to travel dorsally and ventrally at right angles to the large fibers of passage, which projected in the rostral to caudal direction. Some terminal swellings that were quite similar in shape to the calyceal endings of the AVCN and some smaller en passant boutons also could be seen (Fig. 5C,D) in these projections. In the DCN and small cell cap, the terminal fields were composed of sparse networks of fine pre-terminal axons primarily exhibiting small bouton endings (Fig. 5E,F).

Measurements of CN Projection Laminae

Measurements of CN lamina thickness were made in order to determine the distribution of labeled projecting axons across the frequency gradient of each CN subdivision. Figure 6 illustrates the morphometric method for quantitative analysis of the projections. All sections with clear projection laminae were imaged near the center of each projection, and 3 scans were made in each image, using a window positioned at right angles to the projection lamina(e). In Figure 6A, one of the images used to evaluate the PVCN projections in a deafened cat is shown. In addition, the 3 scans from this image and their pixel density plots are illustrated (Fig. 6B). The numerical distributions for all the scans were averaged, and the background density was subtracted until the first negative value occurred in the window to set the threshold level.

Lamina thickness then was calculated as the distance containing 90% of the total pixel density (Fig. 6C). The average lamina thicknesses calculated for the 2 projections shown in Figure 6 are compared to one of the captured images of the projections in Figure 6B. Using this procedure, objective measurements of the CN projections were made relative to the known tonotopic organization of each subdivision of the CN (i.e., estimating the relative distribution of projections across the frequency gradient).

AVCN projections—Injections were made bilaterally in the first group of 5 neonatally deafened animals and in the control, non-implanted cochleae of the deafened animals with cochlear implants (total of 15 cochleae). Double injections were made in all but 2 cochleae, making a total of 25 injections in all. However, only 12 of the CN had labeled projections in the AVCN that were sufficiently intense to be measured, and of these, 10 CN had measurable double projections, making a total of 22 projections that were measured. The AVCN projection laminae in the first group of 5 neonatally deafened animals studied at 3 – 4 months of age averaged 0.254 mm in thickness across the frequency gradient of the nucleus, and the AVCN projection bands in the second group (implanted subjects) averaged 0.258 mm. Moreover, as mentioned previously there was no significant difference in CN size between the two deafened groups. Therefore, the data on CN projection thicknesses have been combined to provide a larger n for statistical comparisons to normal control data. Figure 7A summarizes the data obtained for labeled projections in the AVCN measured in all the deafened subjects, with a mean value of 0.255 mm. This value actually was slightly larger than the corresponding thickness measured for AVCN projections in normal controls (0.223 mm; n= 10 projections, measured in 6 CN), and this difference was statistically significant (one way ANOVA, Tukey Test, p =0.03). Moreover, as stated previously, the CN in the deafened animals was significantly smaller, with a mean maximum cross-sectional area of about 72% of that observed in normal controls. To normalize for CN size, therefore, we divided the AVCN projection thickness in each animal by the dorsal to ventral CN height measured in that subject. The resulting ratio was 0.050 (0.223/4.43) for control subjects. If the CN and its projections in deafened animals were precisely proportionately smaller than normal, then this ratio should be the same in deafened subjects. Since the mean CN height in the deafened subjects was 3.66 mm, then the predicted AVCN projection thickness if proportionate to normal would be $x = 0.050 \times 3.66$ or 0.183mm. Instead, however, AVCN projections in the deafened group actually averaged 0.255 mm, yielding a ratio of 0.069 (0.255/3.66). Thus, when expressed as proportionate difference, the measured AVCN projection thicknesses in neonatally deafened animals were on average about 39% broader than would be predicted if they were proportionate to their smaller nuclear size, and this difference was highly significant (Tukey Test; $p<0.001$).

PVCN projections—PVCN projection laminae were measured in these same two groups of deafened experimental animals each, and projection thickness was virtually identical with mean values of 0.214 mm (neonatally deafened group, bilateral injections, studied at 3–4 months of age) and 0.215 mm (control CN of the deafened/implanted animals). Thus, Figure 7B shows the combined data from a total of 25 PVCN projection laminae measured in 15 CN, with a mean width of 0.215 mm. This value was similar to the value obtained in normal control PVCN projections, which had an average width of 0.205 mm. When normalized for the smaller size of the CN, however, the PVCN projections measured in deafened animals were 26% broader than predicted if they were proportionate to the normal control PVCN projections. As in the AVCN, this difference between the actual measured widths and the expected (proportionate) value was highly statistically significant (Tukey Test, $p<0.001$).

DCN projections—Because the fibers projecting to the DCN are very fine caliber and also have the longest distance to travel from the injection site in the SG, the DCN projections were measurable only in 7 deafened animals (13 projections measured in 9 CN) and had a mean

thickness of 0.223 mm (Fig. 7C). In normal controls (5 projections in 5 CN) the DCN projections averaged 0.188 mm. When normalized for CN size, DCN projections in the deafened animals were 48% broader than predicted if they were proportionate to their normal counterparts, and the difference between the deafened and control groups again was highly significant ($p<0.001$).

It should be noted that the absolute values for both the PVCN and DCN projection thicknesses in deafened subjects were slightly larger than the corresponding normal widths, but these differences were not significant.

Density of Projection Laminae

Figure 8 illustrates the mean pixel densities for projections measured in the AVCN, PVCN and DCN of the neonatally deafened animals as compared to the respective projections in normal control cats. These data demonstrate a significantly lower pixel density for the deafened projections in all three subdivisions of the CN (Student's T-test, unpaired), as expected due to the significant reduction in the spiral ganglion cell population projecting to the CN in the deafened animals.

Projection Separations in Double Injection Cases

As mentioned previously, in several experiments two injections were made in a single cochlea in these experiments. The double injections usually were separated as far as possible within the limits imposed by the round window, and in all cases injections were separated by ≥2 mm. Figure 9A presents data for double-injection cases in which both projections could be measured in all three CN subdivisions and in which both injection sites were also measured. It should be noted that the separation measured between the 2 injection sites in each cochlea was well correlated with the separation between the corresponding CN projections (linear regression correlation; $r^2= 0.91$, $p< 0.001$.) The data in Figure 9A show the absolute separation distances between double CN projections to each subdivision. In the deafened groups, the mean separation distance between labeled AVCN projections from double injections was 0.75 mm, as compared to a separation of 0.78 mm in the control animals. The PVCN projections observed in double-injection cases were separated by 0.36 mm on average in deafened animals vs. 0.40 mm in normal controls. The mean separation between DCN projections in the deafened animals was 0.67 mm as compared to a value of 0.73 mm in controls. Thus, the available data suggest that the projections in both deafened and control groups were separated most widely in the AVCN. By comparison, the average separation of DCN laminae was slightly less than that of the AVCN projections, and the PVCN laminae were the most closely spaced, with a separation of about half that observed for projections in the AVCN and DCN laminae.

In addition, when the CN projection separation distances were normalized by dividing by the injection separation distances in the cochlea for each corresponding double injection case, the proportionate separation was always less in the (smaller) deafened CN than in the normal CN (Fig. 9B). Together these findings suggest that the lamina separation in the CN after neonatal deafening *is proportionate* to the separation observed in normal control subjects and is accounted for simply by the reduced size of the CN. When the intersubject differences in separation of injections sites in the cochlea are taken into account in this manner, the mean separation distances for CN projections were proportionately smaller in all 3 CN subdivisions. Since the deafened CN laminae widths are equal to (or even slightly broader) in absolute values than normal projections, these findings suggesting that double projections are closer together in the deafened animals also support the notion that projections from adjacent cochlear sectors must be more overlapping in the deafened group.

DISCUSSION

The primary goal of this study was to examine the topographic specificity of the neural connections from the cochlear spiral ganglion to the CN in adult animals that had undergone profound hearing loss early in life, and thereby to elucidate the role of normal neuronal activity (normal auditory experience) in development and maintenance of the precise tonotopic maps formed by the primary afferent projections within the CN.

Molecular Mechanisms and the Formation of Tonotopic Maps

It is generally agreed that neural activity is not involved in the ***initial*** formation of topographically ordered sensory pathways, but that is about where the agreement ends with respect to the specific roles of molecular cues and neuronal activity in the development of various topographic maps in the central nervous system (Rubel and Cramer, 2002). In the auditory system several lines of evidence suggest that patterns of connectivity are essentially correctly organized from the time of their initial arrival at target locations. In chicks it has been demonstrated that a tonotopically organized map of the auditory nerve axons projecting within the cochlear nucleus (or nucleus magnocellularis) is present from early embryonic ages, even prior to the formation of synaptic connections by the auditory nerve fibers (Molea and Rubel, 2003). Our previous study in cats demonstrated that a clear tonotopic ordering of SG projections within the CN of kittens examined several days prenatal (Leake et al, 2002). Moreover, studies in mutant mice have demonstrated that at least rudimentary tonotopic connections can form between the cochlea and spiral ganglion even in the absence of differentiated hair cells (Xiang et al., 2003), and that central projections can maintain relatively normal organization despite massive rerouting of fibers in the periphery, as in $Ntf3^{tgBDNF}$ mice in which vestibular fibers project to the cochlea (Fritzsch et al., 2005).

Several other recent studies of the developing auditory system have provided important new information about the molecular mechanisms underlying the assembly of auditory brainstem circuits during embryonic and postnatal development (see Cramer, 2005 for review). Person et al. (2004) demonstrated the role of Eph protein gradients in the formation of the tonotopic connections between the cochlear nucleus and another brainstem nucleus (nucleus laminaris) in the chicken and suggested a possible conserved mechanism for Eph signaling in establishing topographic projections in diverse sensory systems. Additional research specifically examined the expression of Eph proteins in the developing primary afferent auditory nerve projections to the CN analogue (nucleus magnocellularis) in chicks and these findings indicate an important role for the Eph signaling in identifying the appropriate target nuclei and in forming tonotopic projections within the CN in chicks (Siddiqui and Cramer, 2005). Overall, the findings from many recent studies conducted in both chicks and mice, suggest that tonotopic maps initially form through activity–independent processes and that targeting of the neural projections into the inner ear and those to central nuclei are likely guided by specific molecular mechanisms that are distinct from one another (Rubel and Fritzsch, 2002; Fritzsch et al., 2005).

The Role of Neuronal Activity in Development

After this initial formation of neural projections into their target structures, however, many neural systems exhibit refinement of connections during late prenatal and/or early postnatal development. During this period, initial ingrowth of sensory axons may be followed by subsequent regression or “pruning” of the axonal domains resulting in more precise topographic maps of the primary afferent input (e.g., see LeVay et al., 1978; Cowan et al., 1984; Easter et al., 1985; Sachs et al., 1986; Shatz, 1996), and some examples have been reported in the auditory system (Jackson and Parks, 1982; Young and Rubel, 1986; Friauf and Lohmann, 1999; Leake et al., 2002). A number of developmental studies conducted in the visual system have suggested that neuronal activity plays a critical role in this topographic

refinement in mammalian sensory pathways (Shatz, 1996). For example, development of precise adult retinocollicular and retinogeniculate projections from diffuse prenatal projections is thought to be driven by competitive processes. Competition among ganglion cells projecting from the retina (e.g., competition between X and Y axons) influences the size of terminal arbors of retinogeniculate axons (Sur et al., 1984; Friedlander and Tootle, 1990), and interocular competition during development is required for the normal segregation and refinement of projections from the two eyes (LeVay et al., 1978; Sretavan and Shatz, 1986, 1987). More recent studies have suggested that specific spatiotemoral patterns of spontaneous and visual input guide the establishment of precise synaptic connections in the developing visual pathways (Zhou et al., 2003; Chiu and Weliky, 2003), and that the progressive refinement of visual receptive fields in the tectum involves a process of activity-dependent matching of the topography and strength of excitatory and inhibitory connections (Tao and Poo, 2005). Based upon such studies of visual system development, it has been argued that neuronal activity, especially spontaneous activity, plays a critical role in the developmental refinement of topographic organization in all or most mammalian sensory pathways (Schatz, 1990, 1996; Tao and Poo, 2005). However, recent studies showing that topographically precise cortical ocular dominance columns emerge earlier than previously thought (Crowley and Katz, 2000; Crair et al., 2001) and are unaffected by experimentally induced imbalance in retinal activity (Crowley and Katz, 1999), argue that molecular cues may guide highly precise initial column formation, whereas activity-dependent mechanisms are important for maintenance and plasticity of connectional selectivity during the subsequent critical period.

The primary afferent projection from the SG though the auditory nerve and into the CN presents a particularly interesting model for elucidating the role of neuronal activity in the development of topographic organization because of the highly precise tonotopic order of these projections. This organization is established at the level of the hair cells, is maintained within the spiral ganglion, and the projections into the CN form the basis upon which tonotopic organization is established at each successive level of the central auditory system. Each auditory nerve fiber sends collaterals to each of the three CN subdivisions, wherein distinctly specialized terminal arborizations develop. The spatial topography of these respective projections provides the basis for all initial signal processing within the central auditory system. Further, because the cat auditory system is altricial, it provides an excellent opportunity to study the selectivity of neural projections prior to and during the emergence of initial function in the primary afferents. At birth, the cat auditory system is so immature that it is essentially non-functional. Numerous physiological studies have characterized the time course of functional development of the cat auditory system. Behavioral thresholds are extremely high at birth (Foss and Flottorp, 1974; Clements and Kelly, 1978; Olmsted and Villablanca, 1980; Ehret and Romand, 1981), and it is not until several days postnatal that spontaneous activity can be recorded reliably in auditory nerve fibers (Romand, 1984; Walsh et al., 1986). Until P3 or P4, auditory nerve fibers are insensitive to acoustic stimuli (thresholds exceed 120 dB). Auditory nerve fiber thresholds remain high, tuning is broad, spontaneous discharge rates are very low (mean <10 spikes/s) until at least P8 to P10 (Romand, 1984; Dolan et al., 1985; Walsh and McGee; 1986; 1990; Walsh and Romand, 1992). In addition, during the first postnatal week, sound-evoked discharges in the auditory nerve and CN display rhythmic, bursting patterns in response to long-duration acoustic stimuli (Pujol, 1972, Walsh and McGee, 1987; Fitzakerley et al., 1995; 1998; Walsh et al., 1998). This discharge regularity is markedly different from the random interspike intervals seen in adult auditory nerve fibers (Kiang et al., 1965).

Postnatal Refinement of Auditory Nerve Projections to the CN

In our previous studies of the normal development of the spiral ganglion projections to the CN, we used techniques similar to those employed here, first to study these projections in kittens ranging in age from P6-P45 (Snyder and Leake, 1997) and subsequently to examine projections

during the earliest postnatal and late gestation periods (Leake et al, 2002). The results of the first study demonstrated that the topographic specificity of labeled SG projections in each of the three major CN subdividions is as precise in P6 kittens as in adults. This means that the primary afferent projections from the cochlea to the CN are fully refined several days prior to the development of adult-like thresholds and tuning in the auditory nerve. In contrast to the findings in older kittens, our subsequent study demonstrated that auditory nerve projections in neonatal kittens were significantly *broader* in their distributions across the CN frequency gradient than would be expected if they were as precise as adult projections (Leake et al., 2002). In neonates, AVCN projections (normalized for CN size) were more than 50% broader than their adult counterparts, and both PVCN and DCN projections were broader by more than 30%. The decreased topographic selectivity of projections was confirmed by the additional finding that 2 injections that were well-separated in the cochlea resulted in AVCN projections that were *incompletely segregated* and PVCN projections that were *fused* in the youngest subjects studied after C-section at 62 and 63 days gestational age (2 to 3 days prior to the average day of birth). Thus, significant refinement in the primary auditory nerve projections to each CN subdivision occurs during the postnatal period immediately prior to the onset of hearing (i.e., during the period when bursting activity is observed in auditory nerve and CN responses). On the other hand, the tonotopic order of the projections to all three CN subdivisions was clearly evident even in the youngest animals examined. Despite the greater spatial overlap of projections that was demonstrated quantitatively, the degree of selectivity and clear tonotopic order exhibited by the spiral ganglion inputs to the CN at this stage of development was noteworthy (Rubel and Cramer, 2002).

Neonatally Deafened Cats

The neonatally deafened animals included in this study received ototoxic drug injections beginning at birth and continuing for periods of 16–30 days until each subject exhibited a profound hearing loss, as documented by ABR testing. A previous study demonstrated that this protocol results in virtually total hair cell loss throughout the cochlea by the time the ototoxic drug is discontinued, i.e., by the time ABR thresholds are elevated beyond the maximum intensity provided by our system (Leake et al., 1997). As noted previously, cats are born deaf due to the immaturity of their auditory system, and the ototoxic drug administration is initiated immediately. The ototoxic injections had to be continued beyond the first ABR testing at 16 days postnatal in all but 2 subjects, indicating that some high threshold acoustic responses could be elicited at this time. However, all of the animals were profoundly deaf by 30 days postnatal, at about the time that adult-like acoustic sensitivity and tuning develop in the auditory nerve. Thus, these animals clearly were severely deprived from birth, with no normal auditory experience and very little, if any, behaviorally relevant hearing during development and none throughout their subsequent lives. On the other hand, it is not known whether or to what degree spontaneous activity develops and/or persists in the auditory nerve in these deafened animals. Even if some spontaneous activity develops initially, it seems unlikely that it would be maintained for long, given the complete hair cell loss and consequent degenerative changes that occurred in the cochleae of these animals. By the time of study, most of the radial nerve fibers had degenerated and the spiral ganglion cell population was significantly reduced. With respect to this issue, it has been reported that auditory nerve fibers in animals acutely deafened by ototoxic drugs exhibit no spontaneous activity (Hartmann et al., 1987; Parkins, 1989), whereas other studies in chronically deafened cats have reported that they are spontaneously active (Hartmann and Klinke, 1989; Shepherd and Javel, 1997). One problem in chronically deafened animals is that the auditory nerve may be significantly smaller than normal due to SG cell degeneration, and it may be difficult to distinguish between auditory and vestibular neurons, when they are identified by responses to electrical stimuli.

Auditory Nerve Projections in Neonatally Deafened Cats

One of the noteworthy findings in the present study is that the tonotopic organization of the primary afferent auditory nerve (SG) input to the CN clearly developed in neonatally deafened animals and was maintained into adulthood. It is impressive that the CN projections in these deafened animals formed such discrete “frequency band laminae,” with a clear tonotopic gradient and apparently normal orientation from dorsal to ventral within each CN subdivision, despite profound bilateral auditory deprivation and lack of normal auditory input throughout life. Further, projections from 2 injections made in a single cochlea formed segregated projections into each of the CN subdivisions. This maintenance of the topographic specificity of the auditory nerve input to the CN supports the finding in previous electrophysiological studies conducted in animals deafened by this same protocol suggesting that neonatally deafened subjects that did not receive any intervention (such as stimulation from a cochlear implant) exhibited relatively normal tonotopic organization in the auditory midbrain (inferior colliculus) in adulthood (Snyder et al., 1990; Leake et al., 2000)

On the other hand, although these SG projections to CN formed discrete laminae that exhibited clear spatial segregation, the laminae also were proportionately broader than normal in the neonatally deafened subjects. This occurred primarily because the size of the CN was markedly smaller than normal in the neonatally deafened animals. In fact, as estimated by measuring the maximum cross-sectional area of the CN just posterior to the auditory nerve root entry zone, the CN in the deafened group was only about 72% that of normal controls. When CN projection laminae in deafened animals were normalized for the smaller CN size, projections to the three CN subdividisons were all proportionately broader than in normal controls. AVCN projections were 39% broader than normal, and the PVCN and DCN laminae were 26 and 48% broader, respectively, in their relative distributions across the CN frequency gradient. It should be noted that although the quantitative data suggest a larger difference in the DCN projections than in the AVCN and PVCN, we believe that this is an artifact of the labeling method, rather than a real difference in connectional selectivity. Specifically, the fibers to the DCN are very fine and they also have the longest trajectories from the SG, which means that the NB must be transported a longer distance in order to label the DCN projections. Consequently, the yield of DCN projections that were labeled intensely enough to be measured by the objective quantitative methods applied in our experiments was less than for the other subdivisions in *both* normal and deafened groups. Given that there is also some intersubject variability in injection size, we suggest that the more limited number of cases with strong labeling of DCN fibers probably accounts for the relatively small differences between the subdivisions, especially since it seems quite likely that the *larger* injections would tend to better label the fine DCN projections and to result in broader CN projection widths.

The finding of a severe reduction in size of the CN in the neonatally deafened animals, coupled with the evidence that the SG to CN projections in deafened subjects have widths across the frequency gradient that are similar to or even slightly greater than those seen in normal animals, indicates that the projections from adjacent sectors of the SG must be more *overlapping* in these deafened subjects. Thus, the topographic *specificity* of these SG projections to the CN is significantly degraded in these animals that were deafened early in life. The frequency band projections from the cochlea underlie the frequency selectivity in the CN and throughout the central auditory system in the normal brain. If CN projections representing adjacent frequencies in the SG are more overlapping in deafened animals, we can infer that the selectivity of the tonotopic map underlying frequency resolution within the CN also must be less precise (e.g., for stimulation delivered by a multichannel cochlear implant).

Taken together, these findings suggest that neuronal activity (normal auditory experience) may be essential for development and maintenance of the normal connectional precision of the SG projections to the CN into adulthood. The extent to which projections were proportionately

broader in these neonatally deafened animals was very similar to results in normal neonatal kittens examined prior to P6 as described above. When deafness occurs at an early age, the CN fails to grow to its normal adult size, whereas the CN projections mature to normal adult widths, perhaps due to an intrinsic tendency for the SG projections to develop axonal arbors of a specific size. Thus, the significant imprecision in the topographic specificity of the SG to CN projections that is observed during early postnatal development appears to be maintained into adulthood due to the severe atrophy of the CN when the auditory system is severely deprived of normal auditory experience.

In this regard, it should be noted that Schweitzer and Cecil (1992) have previously described the development of the central terminal arbors of individual labeled auditory nerve fibers in the DCN of hamsters. Their findings suggested that terminal fields are relatively restricted at birth and that they expand as the animal matures. This finding is in agreement with our observation in an earlier study that *absolute widths* of projection laminae in all the CN subdivisions in neonatal kittens are actually *smaller* than those in adults (although when the extremely small size of the CN is taken into account, the kitten projections are *proportionately* much broader than those in adults). Together, these findings suggest that the increase in the precision of the cochlear frequency map with maturation may result simply from growth of the CN relative to the size of the auditory nerve terminal arbors, rather than by retraction of initially large arbors or by the correction or elimination of mistargeted axons. The observed initial overlap in the projections to adjacent frequency band laminae sharpens to adult-like precision during the first postnatal week. The absolute widths of CN laminae measured in deafened animals in the present study were very similar to normal adult controls and significantly broader than the laminae in neonates. Therefore, the “refinement” apparently fails to occur in deafened animals because the CN does not grow sufficiently to achieve normal adult size, resulting in *normal-sized projection laminae that are more overlapping in the deafened CN*.

Also relevant to these findings is the work of Ryugo et al, who examined auditory nerve endings in the CN in an animal model of early onset deafness that mimics Scheibe deformity in humans, the congenitally deaf white cat. As in the current study, their results showed well-defined, clearly recognizable endbulds of Held in the AVCN in adult deaf white cats, but the endbulbs had fewer/less complex branches and when examined in transmission electron microscopy the synapses exhibited reduced synaptic vesicle density and hypertrophy of the postsynaptic densities (Ryugo et al., 1997). A subsequent study showed relatively modest alterations in the bouton endings on multipolar cells in the AVCN, with ultrastructural analysis demonstrating a reduction in bouton size in congenitally deaf cats, but no other differences (Redd et al., 2002). Our findings in cats deafened by ototoxic drug administration are consistent with these previous descriptions suggesting that even after congenital deafness of genetic origin, the auditory neurons form well-developed endings that are appropriately specialized for the specific cell types they contact within the CN.

Clinical Implications for Cochlear Implants

The maintenance of the basic tonotopic (or perhaps more appropriately termed “cochleotopic”) organization of the primary afferent input to the central auditory system despite profound hearing loss occurring early in life and prior to the onset of hearing is noteworthy. This finding suggests that if similar principles pertain to the development of the auditory system in humans, the basic cochleotopic organization of central the auditory system is fundamentally intact even in congenitally deaf individuals. Of course, this would be highly advantageous for the application of contemporary cochlear implants (CI) in congenitally deaf individuals, since these devices depend upon the tontopic organization of the auditory nerve to appropriately encode auditory signals across multiple channels of electrical stimulation. Clinical results with

the CI in congenitally deaf subjects generally tend to be poorer than for individuals who have had some prior auditory experience. Nonetheless, many congenitally deaf subjects still receive substantial benefit from their devices, and we suggest (based upon the findings presented here) that the maintenance of the fundamental tonotopic organization of the auditory nerve projections to the central auditory system must underlie that success. At the same time, the degraded frequency resolution observed in neonatally deafened animals suggests that there may be inherent limitations in application of multi-channel cochlear implant stimulation in such congenitally deaf subjects. Specifically, spatial selectivity of stimulation delivered on adjacent CI channels (positioned at set intervals along the cochlear spiral) may be relatively poorer in the congentially deaf CI recipient due to the greater extent of overlap of central axons representing nearby frequencies within the CN. In these circumstances, the CI user may more dependent upon the temporal features of the electrical stimuli delivered by the implant, and it may be advantageous to enhance the salience of such cues, e.g., even by removing some electrodes from the processor to reduce channel interaction, or by using moderate rates of stimulation to enhance the spectral contrasts in the signals.

Acknowledgements

The authors gratefully acknowledge the expert technical assistance of E. Dwan in animal surgery and care.

Grant sponsor: This research was supported by grant 5R01-DC00160 from the National Institute on Deafness and Other Communication Disorders of the National Institutes of Health.

ABBREVIATIONS

ABR
: Auditory brainstem response

AVCN
: Anteroventral cochlear nucleus

CN
: Cochlear nucleus (i.e., AVCN + PVCN + DCN)

DCN
: Dorsal cochlear nucleus

NB
: Neurobiotin

P
: Postnatal day

PVCN
: Posteroventral cochlear nucleus

SG
: spiral ganglion

LITERATURE CITED

Bonham BH, Cheung SW, Benoit G, Schreiner CE. Spatial organization of frequency response areas and rate/level functions in the developing AI. J Neurophysiol 2004;91:841–854. [PubMed: 14534283]

Brawer JR, Morest DK, Kane EI. The neuronal architecture of the cochlear nucleus of the cat. J Comp Neurol 1974;155:251–300. [PubMed: 4134212]

Brugge JF, Reale RA, Wilson GF. Sensitivity of auditory cortical neurons of kittens to monaural and binaural high frequency sound. Hearing Res 1988;34:127–140.

Cant, NB.; Morest, DK. The structural basis for stimulus coding in the cochlear nucleus of the cat. In: Berlin, C., editor. Hearing Science: Recent Advances. San Diego: College-Hill; 1984. p. 371-421.

Chalupa LM, Snider CJ. Topographic specificity in the retinocollicular projection of the developing ferret: an anterograde tracing study. J Comp Neurol 1998;392:35–47. [PubMed: 9482231]

Cheng HJ, Nakamoto M, Bergemann AD, Flanagan JG. Complementary gradients in expression and binding of ELF-1 and Mek4 in development of the topographic retinotectal projection map. Cell 1995;82:371–381. [PubMed: 7634327]

Chiu C, Weliky M. Synaptic Modification by vision. Science 2003;300:1890–1891. [PubMed: 12817134]

Clements M, Kelly JB. Directional responses by kittens to an auditory stimulus. Dev Psychobiol 1978;11:505–511. [PubMed: 689299]

Constantine-Paton M, Cline HT, Debski E. Patterned activity, synaptic convergence and the NMDA receptor in developing visual pathways. Annu Rev Neurosci 1990;13:129–154. [PubMed: 2183671]

Cowan WM, Fawcett JW, O'Leary DDM, Stanfield BB. Regressive events in neurogenesis. Science 1984;225:1258–1265. [PubMed: 6474175]

Cramer KS. Eph proteins and the assembly of auditory circuits. Hearing Res 2005;206:42–51.

Crair MC, Horton JC, Antonini A, Stryker MP. Emergence of ocular dominance columns in cat visual cortex by 2 weeks of age. J Comp Neurol 2001;430:235–249. [PubMed: 11135259]

Crowley JC, Katz LC. Development of ocular dominance columns in the absence of retinal input. Nat Neurosci 1999;2:1125–1130. [PubMed: 10570491]

Crowley JC, Katz LC. Early development of ocular dominance columns. Science 2000;290:1321–1324. [PubMed: 11082053]

Cutforth T, Moring L, Mendelsohn M, Nemes A, Shah NM, Kim MM, Frisen J, Axel R. Axonal ephrin-As and odorant receptors: coordinate determination of the olfactory sensory map. Cell 2003;114:311–322. [PubMed: 12914696]

Dolan DF, Teas DC, Walton JP. Postnatal development of physiological responses in auditory nerve fibers. J Acoust Soc Am 1985;78:544–554. [PubMed: 4031253]

Easter SSJ, Purves D, Rakic P, Spitzer NC. The changing view of neural specificity. Science 1985;230:507–511. [PubMed: 4048944]

Ehret G, Romand R. Postnatal development of absolute auditory thresholds in kittens. J Comp Physiol Psychol 1981;95:304–311. [PubMed: 7229161]

Fekete DM, Rouiller EM, Liberman MC, Ryugo DK. The central projections of intracellularly labeled auditory nerve fibers in cats. J Comp Neurol 1984;229:432–450. [PubMed: 6209306]

Feldheim DA, Kim YI, Bergemann AD, Frisen J, Barbacid M, Flanagan JG. Genetic analysis of ephrin-A2 and ephrin-A5 shows their requirement in multiple aspects of retinocollicular mapping. Neuron 2000;25:563–574. [PubMed: 10774725]

Feller MB, Wellis DP, Stellwagen D, Werblin DFS, Shatz CJ. Requirement for cholinergic synaptic transmission in the propagation of spontaneous retinal waves. Science 1996;272:1182–1187. [PubMed: 8638165]

Fitzakerley JL, McGee J, Walsh EJ. Characteristics of the bursting behavior found in spontaneous activity and in near-threshold discharge response of immature auditory neurons. Neurosci Abstr 1995;21(1): 127.

Fitzakerley JL, McGee J, Walsh EJ. Paradoxical relationship between frequency selectivity and threshold sensitivity during auditory-nerve fiber development. J Acoust Soc Am 1998;103(6):3464–3477. [PubMed: 9637032]

Foss I, Flottorp G. A comparative study of the development of hearing and vision in various species commonly used in experiments. Acta Otolaryng 1974;77:202–214. [PubMed: 4819033]

Friauf E. Tonotopic order in the adult and developing auditory system of the rat as shown by *c-fos* immunocytochemistry. Eur J Neurosci 1992;4:798–812. [PubMed: 12106303]

Friauf, E.; Kandler, K. Cell birth, formation of efferent connections and establishment of tonotopic order in the rat cochlear nucleus. In: Merchan, MA.; Juiz, JM.; Godfrey, DA.; Mugnaini, E., editors. The mammalian cochlear nuclei: Organization and function. NY: Plenum; 1993. p. 19-28.

Friauf E, Lohmann C. Development of auditory brainstem circuitry. Activity-dependent and activityindependent processes. Cell tissue Res 1999;297:187–195. [PubMed: 10470488]

Friedlander, MJ.; Tootle, JS. Postnatal anatomical and physiological development of the visual system. In: Coleman, JR., editor. Development of Sensory Systems in Mammals. New York: John Wiley and Sons, Inc; 1990. p. 61-124.

Fritzsch B, Pauley S, Matei V, Katz DM, Xiang M, Tessarollo L. Mutant mice reveal the molecular and cellular basis for specific sensory connections to inner ear epithelia and primary nuclei of the brain. Hearing Res 2005;206:52–63.

Goodman CS, Shatz CJ. Developmental mechanisms that generate precise patterns of neuronal connectivity. Cell 72/Neuron 1993;10:77–98.

Greenwood, DD. Critical bandwidth in man and some other species in relation to the traveling wave envelope. In: Moskowitz, HR.; Stevens, JC., editors. Sensation and Measurement. Boston: Reidel; 1974. p. 231-239.

Greenwood DD. A cochlear frequency-position function for several –29 years later. J Acoust Soc Am 1990;87:2593–2605.

Hansen MJ, Dallal GE, Flanagan JG. Retinal axon response to ephrin-as shows a graded, concentration –dependent transition from growth promotion to inhibition. Neuron 2004;42:717–730. [PubMed: 15182713]

Hartmann, R.; Klinke, R. Response characteristics of nerve fibers to patterned electrical stimulation. In: Miller, JM.; Spelman, FA., editors. Cochlear Implants: Models of the Electrically Stimulated Ear. Springer-Verlag; New York: 1989. p. 135-160.

Hartmann R, Topp G, Klinke R. Single fiber recordings from the cat auditory nerve with electrical stimulation of the cochlea at different stimulation places. Ann Otol, Rhinol Laryngol 1987;96(Suppl 128):30–31.

Jackson H, Parks TN. Functional synapse elimination in the developing avian cochlear nucleus with simultaneous reduction in cochlear nerve axon branching. J Neurosci 1982;2:1736–1743. [PubMed: 6754881]

Kiang, NYS.; Watanabe, T.; Thomas, EC.; Clark, LF. Discharge patterns of single fibers in the cat's auditory nerve. Cambridge, MA: MIT; 1965.

Kitzes, LM. Development of auditory system physiology. In: Coleman, JR., editor. Development of Sensory Systems in Mammals. New York: Wiley and Sons, Inc; 1990. p. 249-288.

Larsen SA. Postnatal maturation of the cat cochlear nuclear complex. Acta Otolaryngol Suppl 1984;417:1–43. [PubMed: 6598277]

Leake PA, Hradek GT, Snyder RL. Chronic electrical stimulation by a cochlear imlant promotes survival of spiral ganglion neurrons after neonatal deafness. J Comp Neurol 1999;412:543–562. [PubMed: 10464355]

Leake PA, Kuntz AL, Moore CM, Chambers PL. Cochlear pathology induced by aminoglycoside ototoxicity during postnatal maturation in cats. Hearing Res 1997;113:117–132.

Leake PA, Snyder RL. Topographic organization of the central projections of the spiral ganglion in cats. J Comp Neurol 1989;281:612–629. [PubMed: 2708585]

Leake PA, Snyder RL, Hradek G. Postnatal refinement of auditory nerve projections to the cochlear nucleus in cats. J Comp Neurol 2002;448(1):6–27. [PubMed: 12012373]

Leake PA, Snyder RL, Rebscher SJ, Moore CM, Vollmer M. Plasticity in central representations in the inferior colliculus induced by chronic single- vs. two-channel electrical stimulation by a cochlear implant after neonatal deafness. Hearing Res 2000;147:221–241.

LeVay S, Stryker MP, Shatz CJ. Ocular dominance columns and their development in layer IV of the cat's visual cortex: A quantitative study. J Comp Neurol 1978;179:1–51. [PubMed: 8980714]

Liberman MC. The cochlear frequency map for the cat: Labeling auditory nerve fibers of known characteristic frequency. J Acoust Soc Am 1982;72:1441–1449. [PubMed: 7175031]

Limb CJ, Ryug DK. Development of primary axosomatic endings in the anteroventral cochlear nucleus of mice. JARO 2000;1(2):103–119. [PubMed: 11545139]

Maffei L, Galli-Resta L. Correlation in the discharges of neighboring rat retinal ganglion cells during prenatal life. Pro Natl Acad Sci USA 1990;87:2861–2864.

Molea D, Rubel EW. Timing and topography of nucleus magnocellularis innervation by the cochlear ganglion. J Comp Neurol 2003;466:577–591. [PubMed: 14566951]

O'Leary DDM, Wilkinson DG. Eph receptors and ephrins in neural development. Current Opinions in Neurobiol 1999;9:65–73.

O'Leary EE, Yates PA, McLaughlin T. Molecular development of sensory maps: representing sights and smells in the brain. CEll 1999;96:255–269. [PubMed: 9988220]

Osen KK. Cytoarchitecture of the cochlear nuclei in the cat. J Comp Neurol 1969;136:453–484. [PubMed: 5801446]

Osen KK. Course and termination of the primary afferents in the cochlear nuclei of the cat: An experimental anatomical study. Arch Ital Biol 1970;108:21–51. [PubMed: 5438720]

Parkins CW. Temporal response patterns of auditory nerve fibers to electrical stimulation in deafened squirrel monkeys. Hearing Res 1989;41:137–168.

Person AL, Cerretti DP, Pasquale EB, Rubel EW, Cramer KS. onotopic gradients of Eph family proteins in the chick nucleus laminaris during synaptogenesis. J Neurobiol 2004;60:28–39. [PubMed: 15188270]

Prakash N, Vanderhaeghen P, Cohen-Cory S, Frisen J, Flanagan JG, Frostig RD. Malformation of the functional organization of somatosensory cortex inadult ephrin-A5 knock-out mice revealed by in vivo functional imaging. J Neurosci 2000;20:5841–5847. [PubMed: 10908626]

Pujol R. Development of tone-burst responses along the auditory pathway in the cat. Acta Otolaryngol 1972;74:383–391. [PubMed: 4347997]

Redd EE, Cahill HB, Pongstaporn T, Ryugo D. The effects of congenital deafness on auditory nerve synapses: Type I and type II multipolar cells in the anteroventral cochlear nucleus of cats. JARO 2002;3:403–417. [PubMed: 12486596]

Romand R. Functional properties of auditory-nerve fibers during postnatal development in the kitten. Exp Brain Res 1984;56:395–402. [PubMed: 6499969]

Roullier EM, Cronin-Schreiber R, Fekete DM, Ryugo DK. The central projections of intracellularly labeled auditory nerve fibers in cats: An analysis of terminal morphology. J Comp Neurol 1986;249:261–278. [PubMed: 3734159]

Rubel EW, Cramer KS. Choosing axonal real estate: Location, location, location. J Comp Neurol 2002;448:1–5. [PubMed: 12012372]

Rubel EW, Fritzsch B. Auditory system development: Primary auditory neurons and their targets. Ann Rev Neurosci 2002;25:51–101. [PubMed: 12052904]

Ryan AF, Woolf NK. Development of tonotopic representation in the Mongolian gerbil: a 2-deoxyglucose study. Dev Brain Res 1988;41:61–70.

Ryugo DK, Fekete DM. Morphology of primary axosomatic endings in the anteroventral cochlear nucleus of the cat: A study of the endbulbs of Held. J Comp Neurol 1982;210:239–257. [PubMed: 7142440]

Ryugo DK, Ponstaporn T, Huchton DM, Niparko JK. Ultrastructural analysis of primary endings in deaf white cats: Morphologic alteration in endbulbs of Held. J Comp Neurol 1997;385:230–244. [PubMed: 9268125]

Sachs GM, Jacobson M, Caviness VS. Postnatal changes in arborization patterns of murine retinocollicular axons. J Comp Neurol 1986;246:395–408. [PubMed: 3700722]

Sanes DH, Merickel M, Rubel EW. Evidence for an alteration of the tonotopic map in the gerbil cochlea during development. J Comp Neurol 1989;279:436–444. [PubMed: 2918079]

Sato M, Leake PA, Hradek GT. Postnatal development of the organ of Corti in cats: a light microscopic morphometric study. Hearing Res 1999;127:1–13.

Schlagger BL, Fox K, O'Leary DDM. Postsynaptic control of plasticity in developing somatosensory cortex. Nature 1993;364:623–626. [PubMed: 8102476]

Schlagger BL, O'Leary DDM. Early development of the somatotopic map and barrel patterning in rat somatosensory cortex. J Comp Neurol 1994;346:80–96. [PubMed: 7962713]

Schweitzer L, Cecil T. Morphology of HRP-labeled cochlear nerve axons in the dorsal cochlear nucleus of the developing hamster. Hearing Res 1992;60:34–44.

Shatz CJ. Impulse activity and the patterning of connections during CNS development. Neuron 1990;5:745–756. [PubMed: 2148486]

Shatz CJ. Emergence of order in visual system development. Proc Natl Acad Sci USA 1996;93:602–608. [PubMed: 8570602]

Shepherd RK, Javel E. Electrical stimulation of the auditory nerve. I. Correlation of physiological responses with cochlear status. Hearing Res 1997;108:112–144.

Siddiqui SA, Cramer KS. Differential expression of Eph receptors and Ephrins in the cochlear ganglion and eight cranial nerve of the chick embryo. J Comp Neurol 2005;482:309–319. [PubMed: 15669077]

Simon DK, O'Leary DDM. Development of topographic order in the mammalian retinocollicular projection. J Neurosci 1992;12(4):1212–1232. [PubMed: 1313491]

Snyder RL, Leake PA. Topography of spiral ganglion projection to the cochlear nucleus during postnatal development in cats. J Comp Neurol 1997;384:293–311. [PubMed: 9215724]

Snyder RL, Leake PA, Hradek GT. Quantitative analysis of spiral ganglion projections to the cat cochlear nucleus. J Comp Neurol 1997;379:133–149. [PubMed: 9057117]

Snyder RL, Rebscher SJ, Cao K, Leake PA. Effects of chronic intracochlear electrical stimulation in the neonatally deafened cat. I.: Expansion of central spatial representation. Hear Res 1990;50:7–33. [PubMed: 2076984]

Sretavan DW, Shatz CJ. Prenatal development of retinal ganglion cell axons: segregation into eyespecific layers within the cat's lateral geniculate nucleus. J Neurosci 1986;6:234–251. [PubMed: 3944621]

Sretavan D, Shatz C. Axon trajectories and pattern of terminal arborization during prenatal development of the cat's retinogeniculate pathway. J Comp Neurol 1987;255:356–400.

Sur M, Weller RE, Sherman SM. Development of X- and Y-cells retinogeniculate terminations in kittens. Nature Lond 1984;310:246–249. [PubMed: 6462208]

Tao HW, Poo M-m. Activity –dependent matching of excitatory and inhibitory inputs during refinement of visual receptive fields. Neuron 2005;45:829–836. [PubMed: 15797545]

Tolbert LB, Morest DK. The neuronal architecture of the anteroventral cochlear nucleus of the cat in the region of the cochlear nerve root: electron microscopy. Neurosci 1982;7:3053–3067.

Walsh, EJ.; McGee, J. The development of function in the auditory periphery of cats. In: Altschuler, RA.; Bobbin, RP.; Hoffman, DW., editors. Neurobiology of Hearing: The Cochlea. New York: Raven Press; 1986. p. 247-269.

Walsh EJ, McGee J. Postnatal development of auditory nerve and cochlear nucleus neuronal responses in kittens. Hearing Res 1987;28:97–116.

Walsh EJ, McGee J. Frequency selectivity in the auditory periphery: Similarities between damaged and developing ears. Am J Otolaryngol 1990;11:23–32. [PubMed: 2321707]

Walsh EJ, McGee J, McFadden SL, Liberman MC. Long-term effects of sectioning the olivocochlear bundle in neonatal cats. J Neurosci 1998;18(10):3859–3869. [PubMed: 9570815]

Walsh, EJ.; Romand, R. Functional development of the cochlea and the cochlear nerve Chapter 6. In: Romand, R., editor. Development of Auditory and Vestibular Systems 2. Elsevier; 1992. p. 161-219.

Webster WR, Martin RL. The development of frequency representation in the inferior colliculus of the kitten. Hearing Res 1991;55:70–80.

Wong RO, Meister M, Shatz CJ. Transient period of correlated bursting activity during development of the mammalian retina. Neuron 1993;11:923–938. [PubMed: 8240814]

Xiang M, Maklad A, Privola U, Fritzsch B. Brn3c null mutant mice show long-term, incomplete retention of some afferent inner ear innervation. BMC Neurosci 2003;4:2. [PubMed: 12585968]

Young SR, Rubel EW. Embryogenesis of arborization pattern and topography in nucleus laminaris of the chicken brain stem. J Comp Neurol 1986;254:425–459. [PubMed: 3805357]

Zhou Q, Tao HW, Poo MM. Reversal and stabilization of synaptic modifications in a developing visual system. Science 2003;300:1953–1957. [PubMed: 12817152]

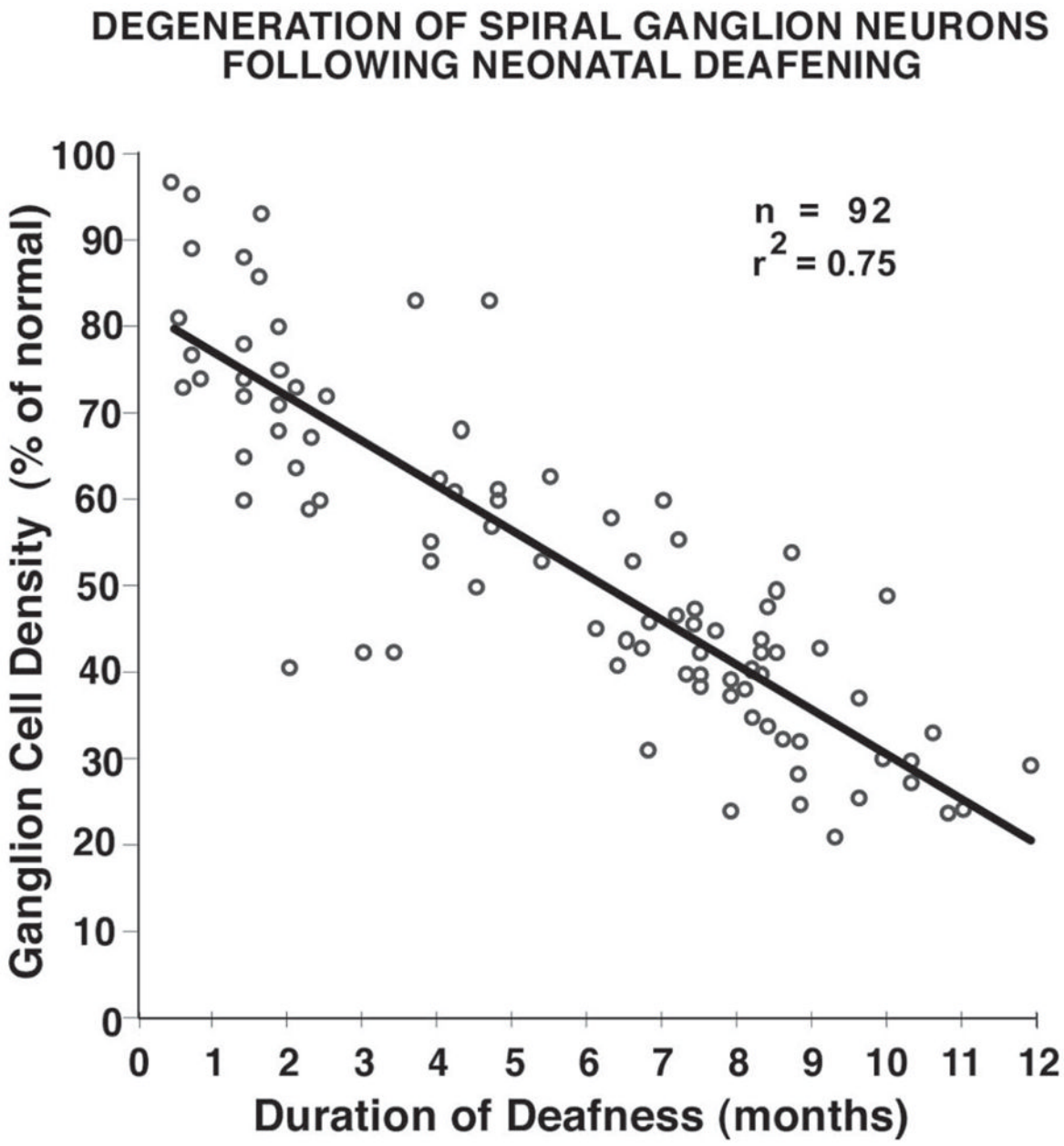

Figure 1.
Survival of spiral ganglion (SG) neurons is shown as a function of duration of deafness for cats deafened immediately after birth by administration of daily injections of the ototoxic drug, neomycin sulfate. The data are presented as mean SG cell density (averaged throughout the cochlea) and expressed as percent of normal. SG survival is strongly correlated with duration of deafness, although there is considerable individual variability for a given duration of deafness.

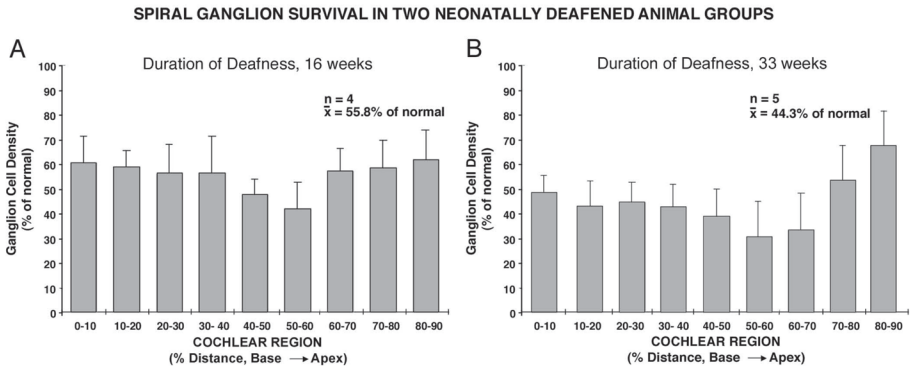

Figure 2.

Spiral ganglion cell densities in the two groups of neonatally deafened cats included in this study are shown as percent of normal for cochlear sectors from base to apex. The first group of 5 neonatally deafened subjects was studied at 3–5 months of age (A). SG data are shown for 4 subjects in this group (because SG data were not available for one of the subjects), and the mean SG density was 55.8% of normal. The second group of 5 neonatally deafened subjects received a unilateral cochlear implant and underwent several months of electrical stimulation of the cochlea, but data from only the contralateral, non-implanted, non-stimulated cochlea and cochlear nucleus are included in the current study. The graph in B shows that SG density in this second group was 44.3% of normal. Error bars indicate standard error of the mean.

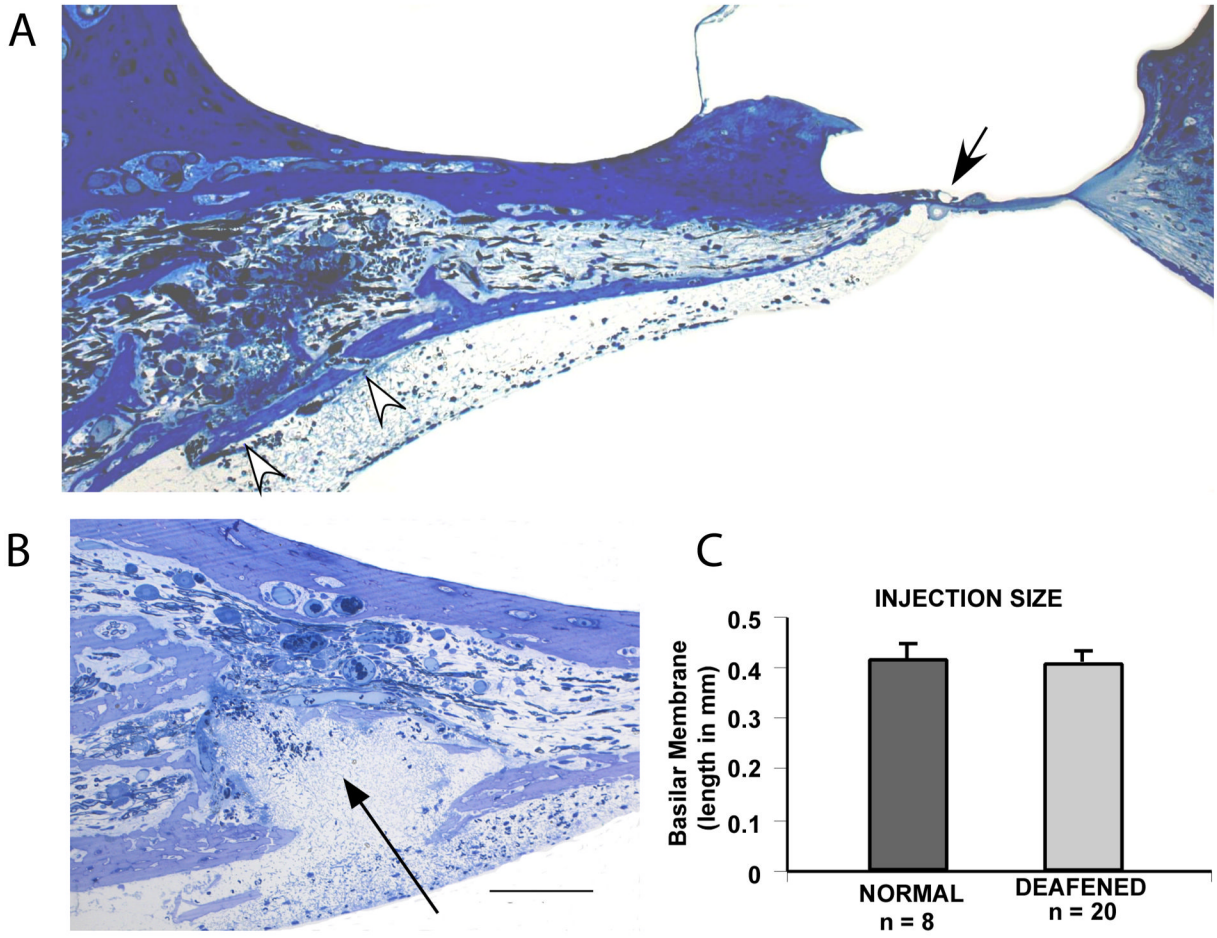

Figure 3.

Images of radial sections through the organ of Corti illustrate the two NB injection sites in cat deafened as a neonate and examined at more than 9 months of age (cat #158). A. This section was taken at about 6 mm from the base (?18 kHz in the normal cochlea) in the region of the apical injection site. Note that the organ of Corti has completely degenerated, collapsing into little more than a squamous cell layer (arrow). Most of the radial nerve fibers that normally innervate the hair cells have degenerated, and very few can be seen within the osseous spiral lamina due to the duration of deafness in this subject. Note, however, that many of the central axons passing into the auditory nerve at the left of the image appear to be intact. Damage to the bone overlying Rosenthal's canal (arrowheads) and a hemorrhage within the canal resulting from the NB injection are evident. B. Section through Rosenthal's canal at about 3.0 mm from the base (? 29 kHz) showing the maximum development of the basal injection site in the same cochlea as in A. The arrow indicates the defect in the osseous spiral lamina through which the glass micropipette was inserted and the injection was made. A small hemorrhage is evident. A few spiral ganglion cells are still recognizable at the top of the ganglion, but most have degenerated. Scale bar = 100 μm. C. Injection site size was determined in serial sections evaluated for evidence of damage to Rosenthal's canal, labeled and damaged spiral ganglion cell somata. Injections in these experiments labeled spiral ganglion neurons innervating cochlear sectors that averaged 412 μm in normal controls and 407 μm in the neonatally deafened animals. Error bars represent standard error of the mean.

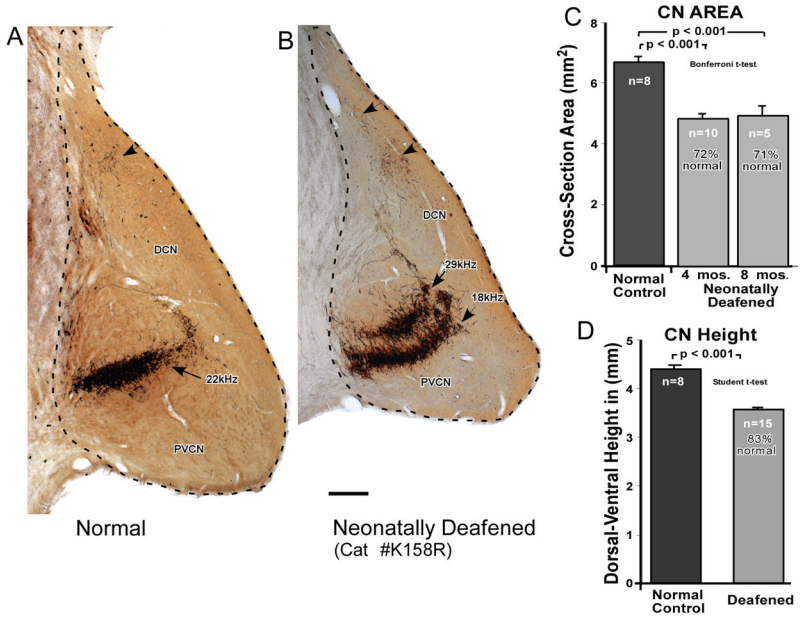

Figure 4.

A. The overall size of the CN was estimated by measuring the cross-sectional area of the CN in the single largest section taken just posterior to the entrance of the auditory nerve, and tracing the perimeter, as illustrated here in normal adult (A) and neonatally deafened (B) subjects. Scale bar = 0.4 mm. C. The mean CN area was then calculated for the normal adult control group (6.83 mm2) and for the two deafened groups. The two deafened groups had CN cross-sectional areas that were virtually identical to each other (4.84 mm2 for the neonatally deafened group studied at 4 months of age and 4.94 mm2 for the neonatally deafened group studied at about 8 months of age), but the deafened CN were markedly smaller than normal, measuring only about 72% that of normal controls. This difference was highly statistically significant (Student's t-test, unpaired). D. The dorsal-to-ventral height of the CN was measured to provide a single-dimensional scaling factor that was used to normalize the thickness of SG projections for the smaller CN size in deafened subjects. The CN height was significantly reduced in the deafened group. Error bars indicate standard error of the mean.

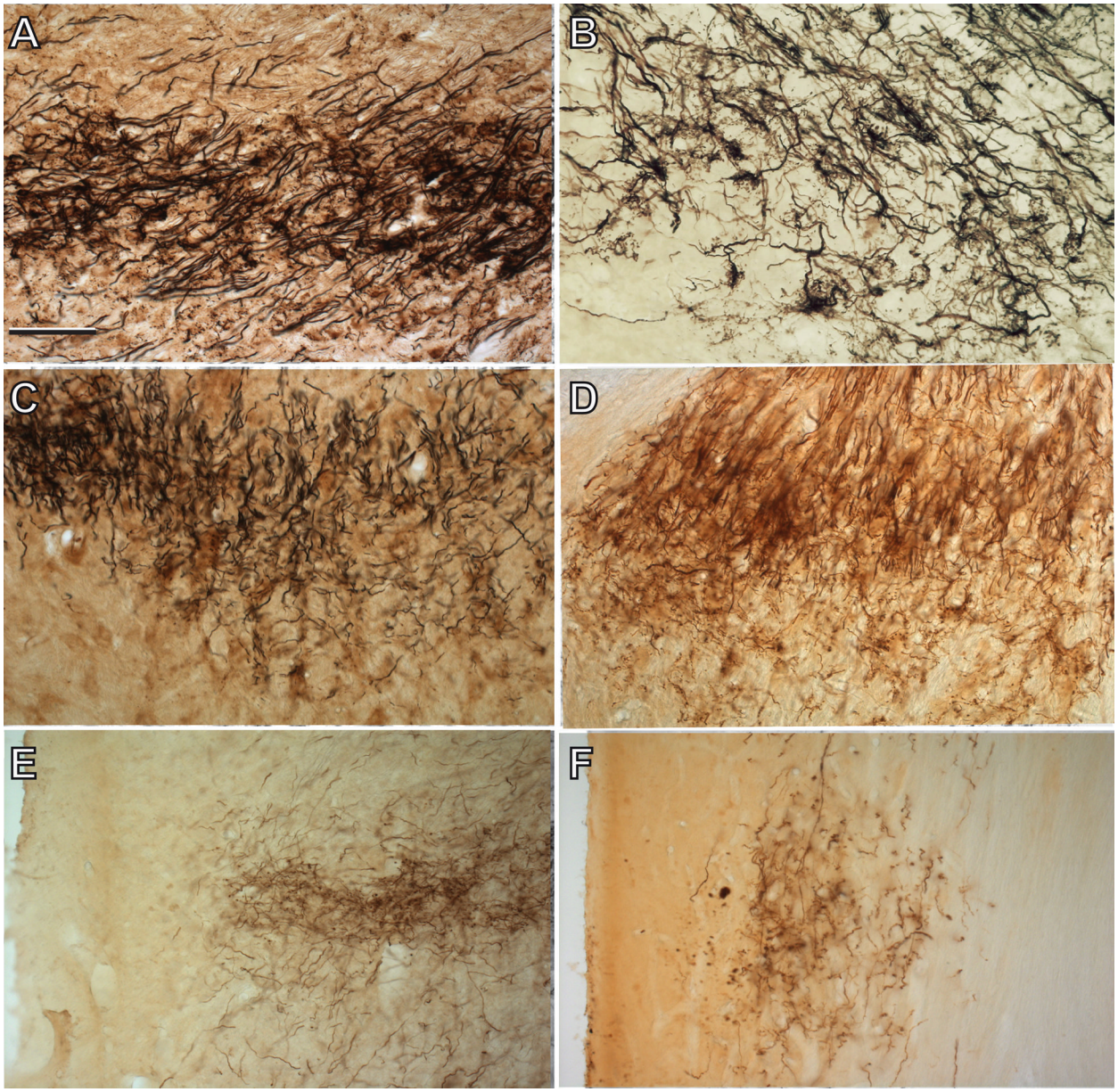

Figure 5.

A,B. NB labeled auditory nerve fibers in the AVCN projection lamina in a normal adult cat (A) and in a neonatally deafened cat (B) examined at about 8 months of age (K169). Arrows indicate auditory nerve calyceal endings, which appear to be relatively normal light microscopy, although not as dense as normal. C,D. NB labeled auditory nerve fibers in the PVCN of a normal adult (C) and in another neonatally deafened subject (D) examined at more than 9 months of age (K158) and for which the cochlear injection sites are illustrated in Figure 3. The image illustrates the complexity and density of the neuropil in PVCN and the fine string endings, which are seen passing ventrally from the main projection lamina along its caudal extent. E,F. Labeled auditory nerve fibers in the DCN projection lamina of a normal adult cat (E) and a deafened subject (F), illustrating the fine caliber of labeled auditory nerve fibers and terminals in this region. Scale bar in A = 100 μm and indicates magnification for all micrographs.

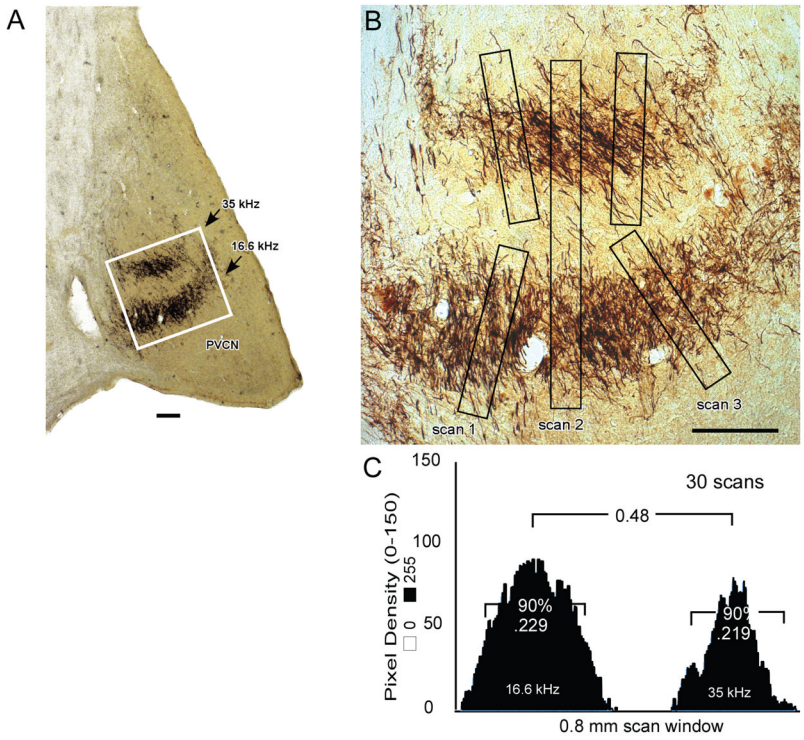

Figure 6.

A,B. CN projection thickness was estimated by determining the mean pixel density in windows of 0.5 mm (25 pixels) by 0.04 mm (200 pixels) with the scan window positioned orthogonal to the projection lamina (e.g., scans 1 and 3 in B). The scans were always executed beginning at the low frequency side of each lamina. In each image, 3 scans were made orthogonal to each projection lamina. The section illustrated is taken from a deafened animal (K169) that was studied at about 8 months of age. Outlined area in A is equal to 1 mm2 and is shown at higher magnification in B. C. For each projection, scans from all sections were averaged. Threshold level was set by subtracting background density until the first negative value occurred in the window. The average plot was normalized, and projection thickness was calculated as the distance containing 90% of the total pixel density. This value was 0.219 mm for the 35 kHz (upper) projection and 0.229 mm for the 16.6 kHz (lower) projection to the PVCN illustrated here. The separation between 2 laminae was determined in a larger scan window of 0.5 mm by 0.8 mm as illustrated by scan 2 in B and measuring the distance between the two maxima in the averaged pixel density plot as shown in C. Scale bars in A and B = 200 μm.

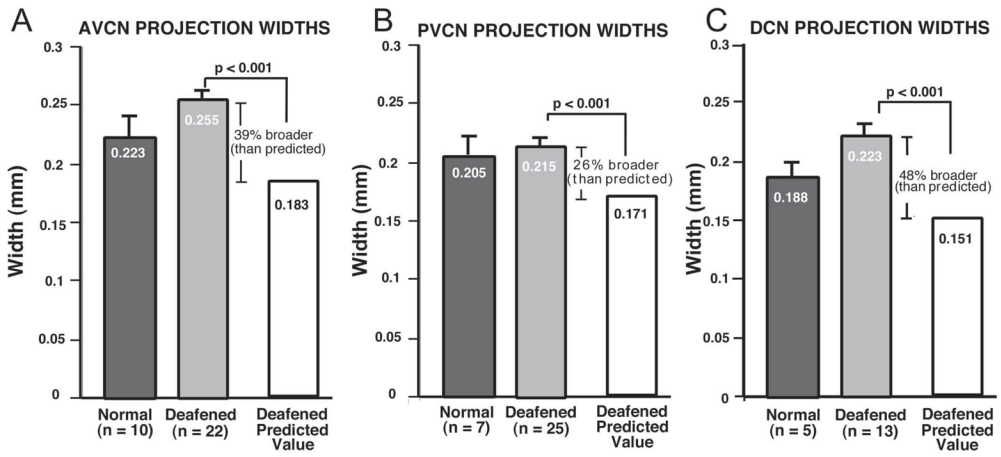

Figure 7.

A. The data for mean thickness of projection laminae in the AVCN are shown, as measured in sections from normal adult controls (black bar) and for all neonatally deafened animals (gray bar). The mean projection thickness in deafened subjects (255 μm) actually was slightly greater than normal (223 μm). Moreover, when the normalized value predicted for the smaller deafened CN was calculated (i.e., if laminae in the deafened CN were precisely proportionate to those in the normal CN), the predicted value was 183 μm. Thus, the AVCN projections in the deafened animals were 39% broader than predicted if they were proportionate to the projections in normal control subjects. B. Data are shown here for the PVCN projections in the same groups. The PVCN projection laminae measured in normal controls had a mean thickness of 205 μm, and the PVCN projection thickness measured in deafened animals was very similar, with an average value of 215 μm. When normalized for the smaller size of the CN in the deafened group, however, the predicted PVCN projection thickness was 171 μm. Thus, the measured PVCN projections thickness in deafened animals was proportionately 26% broader than in normal controls. C. The DCN projection laminae measured in normal controls averaged 188 μm. The absolute mean values for projections in deafened subjects were slightly larger than normal, with an average of 0.223 mm. When normalized for CN size, the expected DCN projection thickness for the deafened group was 0.151 mm. Thus, DCN projections in the deafened animals were 48% broader than projections in controls, when scaled relative to CN size. Note that the absolute values for both the PVCN and DCN projection thickness in deafened subjects were slightly larger than the corresponding values in normal controls, but these differences were not significant. The error bars indicate standard error of the mean.

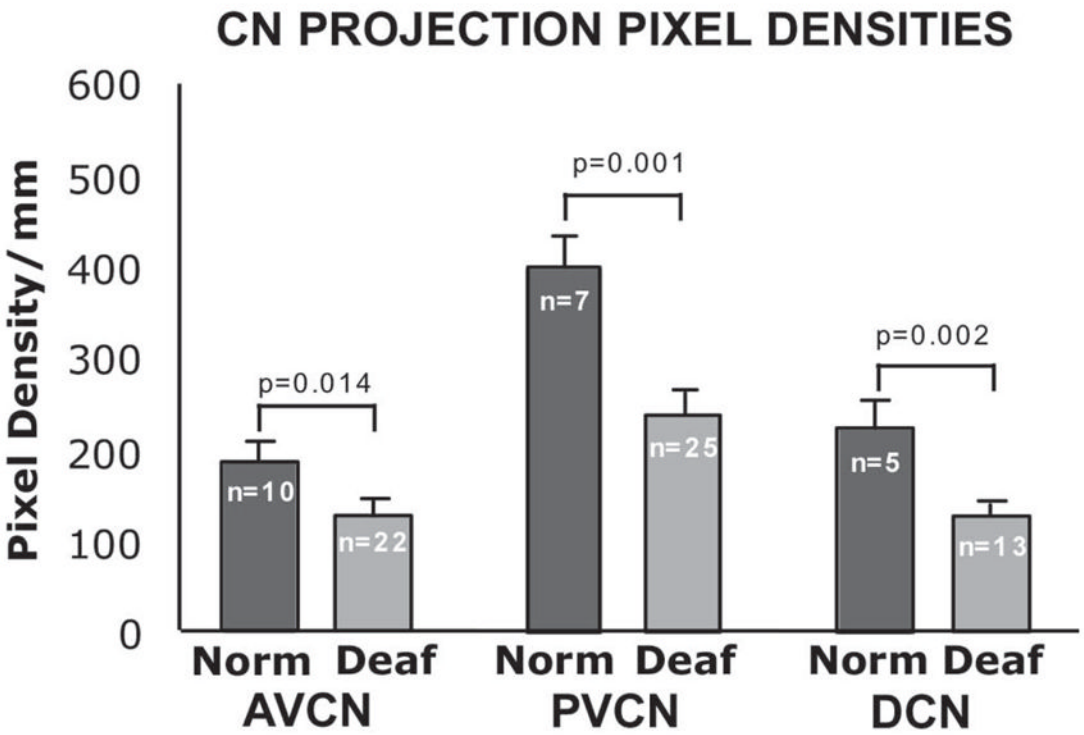

Figure 8.
Average pixel density values for all scans are compared for normal controls and deafened groups in each of the CN subdivisions. In all three subdivisions of the nucleus, AVCN and PVCN and DCN, pixel densities are significantly reduced in the deafened subjects as compared to normal controls. Error bars represent standard error of the mean.

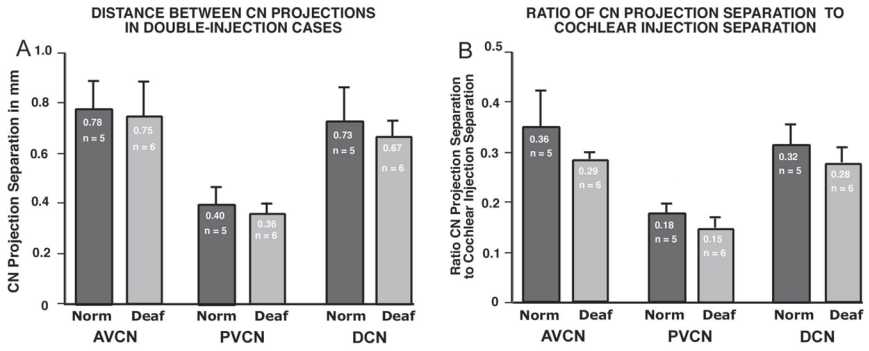

Figure 9.

A. Mean separation distance between CN projection laminae is shown for cases in which two successful injections were made in a single cochlea, and projections to all 3 CN subdivisions were sufficiently intense to be measured. Data shown compare absolute values for separation distances in AVCN, PVCN and DCN in control and neonatally deafened groups. The separation in AVCN and DCN projections was about double that between the corresponding PVCN projections. B. The data from A are normalized for the separation between injection sites by dividing the absolute CN projection separation values by the separation distances for the corresponding cochlear injection sites. When the intersubject variability is taken into account in this manner, the proportionate values were always smaller in the deafened CN. Since the CN laminae in deafened animals are equal in thickness to projections in the normal group, this finding that projections are closer together in the deafened group supports the suggestion that the CN projections from adjacent cochlear sectors must be more overlapping in the deafened group.

Table 1

INDIVIDUAL SUBJECT DATA

Cat #	Neomycin # days	Age at Initial Stimulation (weeks)	Age at Study (weeks)	# of Injections Left,Right	SG Density (% of normal)	CN: max X-Sect. Area (mm^2)
			NEONATALLY DEAFENED			
K110	16	--	14	2,2	42.5	4.94
K112	16	--	16	2,1	35.3	4.25
CD384	30*	--	16.5	2,2	83.0	4.71
CD387	30*	--	17	2,2	55.2	5.32
CH537	20	--	21.5	1,1	NA	4.78
			NEONATALLY DEAFENED, CONTRALATERAL TO COCHLEAR IMPLANT			
K154	21	6	40	--,1	40.1	5.29
K158	19	7	41	--,2	37.1	4.39
K160	19	6	34	--,2	37.3	4.05
K163	19	6	20	--,2	84.5	6.08
K169	19	8	33	--,2	23.7	4.89
			NORMAL ADULT CONTROLS			
423	--	--	--	3,3	--	6.62
596	--	--	--	2,2	--	7.06
654	--	--	--	2,2	--	7.21
944	--	--	--	1,1	--	6.42

* 2 subjects had measurable ABR thresholds after 24 days of 60 mg/kg/d neomycin, so the neomycin was increased to 70 mg/kg for the final 6 days after which both animals exhibited profound hearing loss.